Modeling of Transmission Characteristics Across a Cable-Conduit System

Varun Agrawal, *Student Member, IEEE*, William J. Peine, *Member, IEEE*, and Bin Yao, *Senior Member, IEEE*

***Abstract*—Many robotic systems, like surgical robots, robotic hands, and exoskeleton robots, use cable passing through conduits to actuate remote instruments. Cable actuation simplifies the design and allows the actuator to be located at a convenient location, away from the end effector. However, nonlinear frictions between the cable and the conduit account for major losses in tension transmission across the cable, and a model is needed to characterize their effects in order to analyze and compensate for them. Although some models have been proposed in the literature, they are lumped parameter based and restricted to the very special case of a single cable with constant conduit curvature and constant pretension across the cable only. This paper proposes a mathematically rigorous distributed parameter model for cable-conduit actuation with any curvature and initial tension profile across the cable. The model, which is described by a set of partial differential equations in the continuous time-domain, is also discretized for the effective numerical simulation of the cable motion and tension transmission across the cable. Unlike the existing lumped-parameter-based models, the resultant discretized model enables one to accurately simulate the partial-moving/partial-sticking cable motion of the cable-conduit actuation with any curvature and initial tension profile. The model is further extended to cable-conduit actuation in pull–pull configuration using a pair of cables. Various simulations results are presented to reveal the unique phenomena like backlash, cable slacking, the interaction between the two cables, and other nonlinear behaviors associated with the cable conduits in pull–pull configuration. These results are verified by experiments using two dc motors coupled with a cable-conduit pair. The experimental setup has been prepared to emulate a typical cable-actuated robotic system. Experimental results are compared with the simulations and various implications are discussed.**

***Index Terms*—Cable-conduit actuation, cable compliance, friction, pull–pull configuration, surgical robot.**

I. Introduction

SURGICAL robots often utilize cable-conduit pairs in a pull–pull configuration to actuate the patient-side manipulators and slave instruments [2], [3]. Cable transmissions are preferred because they can provide adequate power through narrow tortuous pathways and allow the actuators to be located safely away from the patient. Cables are light weight and cost effective and greatly simplify the transmission. Cable-conduit actuation, which is also sometimes known as tendon sheath, or Bowden cable actuation, is also used in many robotic hands [4]–[6], as well as colonoscopy devices [7], [8]. To develop power dense yet ergonomic actuation for wearable interfaces, cable actuation is also used in exoskeleton robots [9]–[11]. The control of these systems, however, is challenging due to cable compliance and friction within the conduit. These nonlinearities introduce significant tension losses across the cable and give rise to motion backlash, cable slack, and input-dependent stability of the servo system [12], [13]. In the absence of a transmission model for the cable-conduit system, these nonlinear behaviors are not accounted for [9]–[11], leading to poor system performance. Although various physical measures are adopted including using PTFE-coated steel cables sliding in *slightly preloaded* Kevlar-reinforced housings [10] and keeping the cable-wrapping angles and pretension to low levels, they can only improve the system performance to a certain degree. Beyond that, one has to rely on effective control algorithms to improve the performance, which stresses the importance of developing a model for the transmission characteristics. This paper develops a model for the transmission characteristics in cable-conduit mechanisms to effectively analyze such a system.

Kaneko *et al*. [12] performed experiments on torque transmission from the actuator to the finger joint using a pair of cables passing through conduits. However, no analytical model was developed. These experiments assumed a large value of pretension in the cable to avoid any slacking. Since friction forces are directly dependent on cable pretension, it leads to a tradeoff between tension losses and cable slacking. Thus, cable slacking is an important phenomenon that should be addressed. Later on, the authors developed a model for a single cable passing through the conduit of fixed constant curvature with a given constant pretension throughout the cable [14], [15]. Based on the model, they analytically calculated the equivalent cable stiffness for a single cable. Furthermore, the authors proposed a lumped-mass numerical model for tension transmission across the cable. Through their model, they demonstrated the cable-conduit system display direction-dependent behavior and, hence, cannot be treated as a simple spring. However, their model essentially assumes that all points on the cable have the same initial pretension of a constant value and, as such, cannot consider the general behavior of a cable-conduit transmission, where the initial tension depends on the spatial positions. The calculation of last moving point when using multiple-lumped elements also assumes the same constant pretension across all elements, which essentially

Manuscript received December 10, 2009; revised April 27, 2010; accepted July 28, 2010. This paper was recommended for publication by Associate Editor A. Albu-Schäffer and Editor W. K. Chung upon evaluation of the reviewers' comments. This work was supported by Meere Company, South Korea. This paper was presented in part at the IEEE International Conference on Robotics and Automation, Pasadena, CA, 2008 [1].

The authors are with the School of Mechanical Engineering, Purdue University, West Lafayette, IN 47906 USA (e-mail: vagrawal@purdue.edu, peine@purdue.edu, byao@purdue.edu).

Color versions of one or more of the figures in this paper are available online at http://ieeexplore.ieee.org.

Digital Object Identifier 10.1109/TRO.2010.2064014

ignores the spatial dependence of the tension transmission across the cable and prevents accurate study of some of the unique phenomena associated with the cable-conduit actuation mechanisms, such as partial moving/partial sticking. In practice, due to the presence of friction, the residual tension or initial tension profile depends on the time history of past applied forces and cannot be assumed to be uniform across the cable. Moreover, in many applications, like surgical robots and exoskeletons, the conduit curvatures are path dependent, and thus, the model cannot be applied directly for these applications. Because of these issues, the assumption of constant curvature and a predetermined constant pretension across the entire cable severely limits the usefulness of the model. Palli and Melchiorri [16], [17] further refined the model using a dynamic Dahl's friction model instead of the simple Coulomb friction model but made the same assumptions of constant pretension and curvature for the lumped-element models. Furthermore, all these existing models only focus on power transmission using a single cable conduit and, therefore, cannot address the unique phenomena of cable slacking and cable interaction associated with the systems using a pair of cables for power transmission, like the ones studied in this paper.

Instead of using the lumped-mass analysis, this paper first develops an exact, continuous time-domain model described by a set of partial differential equations (PDE's), which is applicable to cable-conduit systems with any pretension and curvature profiles. In addition, this paper considers the complex interaction between a pair of cables in pull–pull. The exact infinite-dimensional model is then discretized to generate effective numerical simulation algorithms for motion and power transmissions. This can be used to solve the nonlinear system response to predict cable slacking and overall transmission characteristics of the system. The model is validated through experiments.

Unlike the single-cable system discussed in detail in the earlier research, the use of pair of cables induces cable interaction leading to behavior that is completely absent in the prior cases. While the previous models have been developed using lumped-mass analysis with inertia, our work uses the exact distributed system dynamics to generate the discretized model for analysis and simulation, although the cable inertia is neglected. Furthermore, the phenomenon of partial cable segment, which causes the cable interaction, can be explained. The approximation errors in the discretization process have been clearly laid out as well. Moreover, while only force transmission has been analyzed in previous research, motion transmission has also been presented here, which is particularly important for surgical devices, which are usually operated in position control mode. In the following sections, the setup of the problem is discussed followed by details of the proposed model and the simulation results. The methodology of experiments is outlined, and experimental results are presented and compared with the simulation results.

II. Motivation and Experimental Setup

In cable-drive robots, the slave manipulators are mechanically actuated using cable drives passing through a thin tube or conduit. Nonlinearities are introduced in motion transmission due to the friction forces between the cable and the conduit. Moreover, tension losses across the cable necessitate much higher actuating forces for relatively small loads. While high pretension is desired to avoid cable slacking, it comes with a drawback of higher friction forces. However, lower pretension leads to cable slacking. Thus, a tradeoff is required between cable slacking and large actuation forces. Since it is difficult to place sensors at the distal ends of the highly miniaturized instrument, such as in a surgical robot, the position and applied forces of the tool tip are difficult to estimate and control. Hence, the resultant accuracy of the system is extremely poor, as compared with industrial robots. In surgical robots, this results in continuous adjustment of the actuating input by the human in the loop, thereby potentially affecting the performance of the surgeon. The objective of this research is to model cable actuation in such a system and characterize the force and motion transmission from the actuator to the load. Ultimately, these models can be used to improve the control strategy of the system.

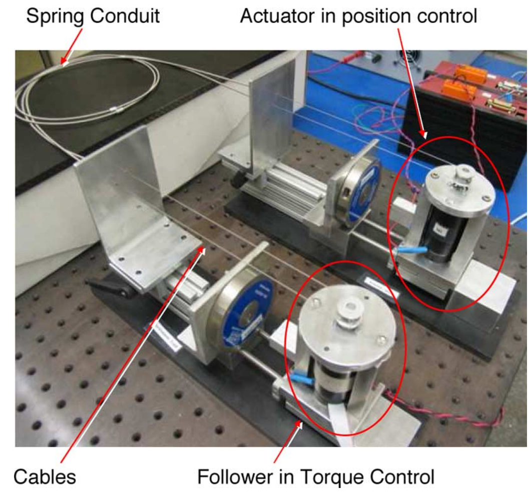

Fig. 1. Experimental setup.

A typical load actuation system of a cable actuated robot has been emulated in the experimental setup shown in Fig. 1. A schematic of the setup is shown in Fig. 2. A two-cable pull–pull transmission is used, actuated with two brushed dc motors mounted on linear slides. The first motor is controlled as the input or the drive motor, while the second motor simulates a passive load or environment. Each cable passes through a flexible conduit and is wrapped around pulleys attached to each of the dc motors. The tightly wound spring wire conduits are fixed at each end using two plates attached to the same platforms on which the linear slides are mounted. This way, the platforms holding the plates are free to move in space, and applying a tension in the cable is counteracted by a compression in the conduit with no forces being transmitted through the ground. The cable and the conduit, therefore, act as springs in parallel.

The actuator or the drive motor is run in position control mode, while the follower motor is run in torque control mode. The load is simulated as a torsional spring such that the restoring torque applied by the motor is proportional to the angle of rotation.

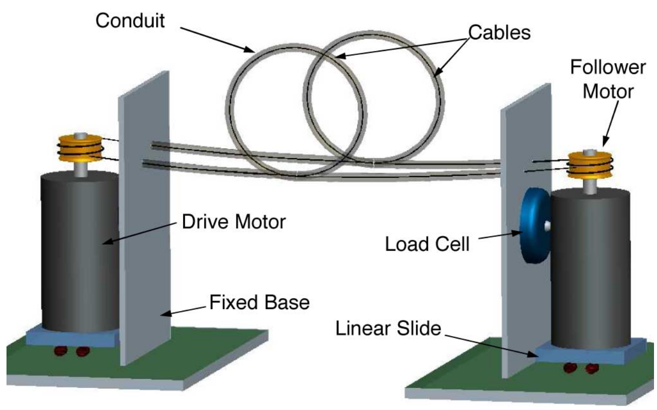

Fig. 2. Model of the experimental setup.

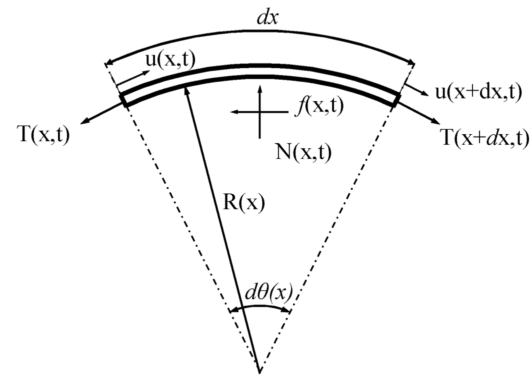

Fig. 4. Forces balance diagram of cable element.

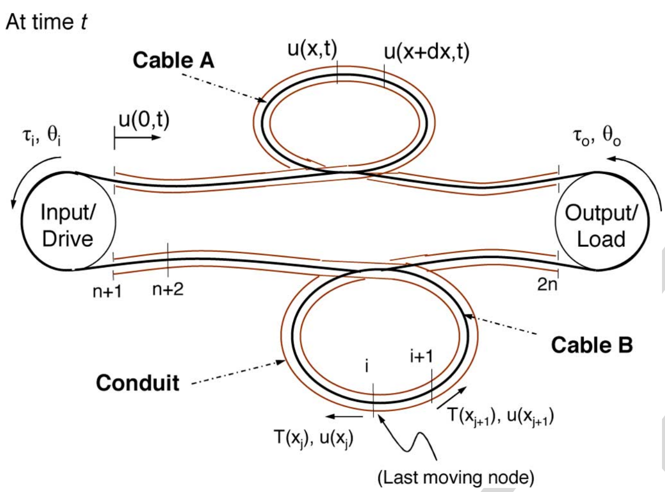

Fig. 3. Motion of the cable element.

Encoders are used to measure the angular rotation of the two motors. The current flowing across the two motors is used to estimate the torque applied by the pulley, which is proportional to the difference in the two cable tensions on each side. The sum of the tensions being applied by the two cables on each motor is measured using load cells mounted between the linear slide and conduit-termination plate. Using the torque values and the load cell measurements, tension at the two ends of each cable can be calculated.

III. Dynamic Model

A. System Governing Equations

Consider the setup shown in Fig. 3, where two flexible cables, i.e., cable A and cable B, pass through fixed conduits of predefined curvature $R(x)$, where x denotes the position along the conduit. At $t = 0$, actuator starts to move the cables. To model the motion of the cable, we make the following assumptions.

1) Inertia effects in the cable can be neglected.
2) The cable is restricted to move along conduit (no transverse motion).
3) Interaction between the cable and the conduit is through a normal force and friction (Coulomb friction).
4) Constitutive behavior of the cable is assumed to be elastic, defined by the standard Hooke's law.

When at relaxing state (i.e., no tension) without slacking, points on the cable can be uniquely indexed by the conduit position x. For the point on the cable indexed by x, let $u(x,t)$ denote its axial displacement at time t, and let $T(x,t)$ be the corresponding axial tension of the cable. For notational simplicity, in the following, the partial derivative of a function $T(x,t)$ with respect to the spatial variable x will be denoted by $T'(x,t)$ and the partial derivative with respect to the time variable t by $\dot{T}(x,t)$.

To obtain the dynamic model of the motion and force transmitted through the cable, consider the movement of an infinitesimal cable segment $[x, x + dx]$, as shown in cable A of Fig. 3 with an enlarged view shown in Fig. 4. In Fig. 4, $N(x,t)$ denote the normal force between the cable and the conduit. $f(x,t)$ is the frictional force acting on the cable. For this infinitesimal segment, the radius of curvature can be assumed to be constant, given by $R(x)$, and the infinitesimal angle $d\theta\,(x)$ shown in Fig. 4 is related to dx by $dx = R(x)d\theta(x)$. As there is no cable movement along the radial direction of the conduit, through the force balancing equation, the normal reaction force acting on this infinitesimal cable element is related to the tensions at the two ends by

$$N(x,t) = T(x,t)\sin\left(\frac{d\theta(x)}{2}\right) + T(x+dx,t)\sin\left(\frac{d\theta(x)}{2}\right) \approx T(x,t)d\theta(x). \tag{1}$$

Thus, from the Coulomb friction model, we know that

$$|f\,(x,t)| \;\le\; \mu N\,(x,t) = \;\mu T\,(x,t)\,d\theta\,(x) = \mu T\,(x,t)\,\frac{dx}{R\,(x)}. \tag{2}$$

As the inertia of the cable is neglected, the force balance equation applies to the axial direction of the conduit (i.e., the cable movement direction) as well. Therefore, when the net axial tension force $T(x{+}dx,t) - T(x,t) = T'(x,t)dx$ is less than the right-hand side of (2), i.e., $|T'(x,t)| < \mu T(x,t)/R(x)$, the cable segment will not move, and the actual friction $f(x,t)$ has the same magnitude as the net axial tension force, i.e.,

$$\dot{u}(x,t) = 0 \quad \text{and} \quad f(x,t) = T'(x,t)dx. \tag{3}$$

On the other hand, when the cable segment moves due to the net axial tension forces, friction will be at its maximum value, as given by (2), i.e., $f(x,t) = (\mu T(x,t)/R(x))\mathrm{sign}\,(\dot{u}(x,t))\,dx$. Thus, from the force balance equation

$$T'(x,t)dx \;=\; \frac{\mu T(x,t)}{R(x)\mathrm{sign}}\,(\dot{u}(x,t))\,dx \quad \text{ when } \dot{u} \neq 0. \quad (4)$$

To calculate the cable strain along the conduit path $u'(x,t)$, it is assumed that, when stretching, Hooke's law of elasticity can be used by modeling the cable as a linear spring with stiffness *K*, and when compressing or cable slacking, no force transmitted through the cable. Since the cable and the conduit act in parallel, K is the combined stiffness of the system. Thus

$$\begin{aligned} &T(x,t) = K\,u'(x,t) \quad \text{when} \quad u'(x,t) > 0\\ &T(x,t) = 0 \quad \text{when} \quad u'(x,t) \le 0\\ &\text{where} \quad \frac{1}{K} = \frac{1}{K_{\text{cable}}} + \frac{1}{K_{\text{conduit}}}. \end{aligned} \quad (5)$$

Combing (3)–(5), the overall distributed dynamic model of the motion and tension across the cable is described by the following sets of PDEs:

$$\begin{aligned} &\text{when} \;\; u'(x,t) > 0, \;\; T(x,t) = K\,u'(x,t) \text{ and}\\ &\quad \text{i)} \quad u''(x,t) - \frac{\mu}{R(x)}u'(x,t)\mathrm{sign}\,(\dot{u}(x,t)) = 0\\ &\qquad\qquad \text{if } |u''(x,t)| = \frac{\mu}{R(x)}u'(x,t)\\ &\quad \text{ii)} \quad \dot{u}(x,t) = \;0, \qquad \text{otherwise}\\ &\text{when} \;\; u'(x,t) \le 0\\ &\quad \text{iii)} \quad T(x,t) = 0. \end{aligned} \quad (6)$$

Aside from the aforementioned governing equations, to calculate the motion and tension transmission across the cable, one needs the initial conditions and the boundary conditions as well. Thus, to be able to precisely describe the cable dynamic behavior, it is absolutely necessary to specify the initial cable displacement profile $u_0(x)$, i.e.,

$$u(x,0) = u_0(x) \quad (7)$$

and the boundary conditions of the cable at the two ends, depending on the environment to which the cable is attached. For example, consider a cable with the end at $x = 0$ connected to an environment having a predefined movement of $g_{id}(t)$ and the other end at $x = L$ fixed to a stiff environment having a stiffness of K_e; then, noting (7), the boundary conditions for solving the cable movement would be

$$\begin{aligned} &u\,(0,t) = g_{id}\,(t)\\ &u\,(L,t) = -\frac{1}{K_e}T\,(L,t) = -\frac{K}{K_e}\,u'(L,t). \end{aligned} \quad (8)$$

Remark 1: In the earlier development of the mathematically rigorous distributed parameter model for cable-conduit actuation, no restriction is put on the curvature of the conduit, i.e., $R(x)$ could be any function. This is in contrast with the previous work in [14]–[17], where constant curvature is assumed across each cable segment. Furthermore, no restriction is put on the initial cable displacement profile $u_0(x)$, and thus, the initial tension profile of $T\,(x,0) = K\,u'\,(x,0) = K\,u_0'\,(x)$ (assume that $u_0'\,(x) \ge 0$). *It is noted that all the previous work [14]–[17] assume a constant initial tension profile of* $T\,(x,0) = T_0$*, which is hardly true in reality due to the distributed friction effect across the cable.* Thus, although some of the discretized equations on the tension transmission for a particular segment introduced in the following section may look somewhat similar to those in [14]–[17], the overall modeling process is fundamentally different from the previous work. In addition, cable slacking is explicitly taken into account in the proposed model, which cannot be addressed using previous work.

B. Discretized Model

Since it is impossible to analytically solve the PDEs (6), in practice, discretized element models based on these governing equations are obtained for realistic computer simulations, which is the subject of this section. As shown by cable B in Fig. 3, the each cable is divided into n cable segments, with nodes at $x_1 = 0$, $x_2 = \Delta x_1$, $x_3 = x_2 + \Delta x_2, \ldots,$ and $x_n = x_{n-1} + \Delta x_n = \sum_{i=1}^{n} \Delta x_i = L$. The displacement and tension of the two ends of each segment will be calculated at discrete time instants using the discretized elemental equations as follows.

Consider the ith cable segment between nodes i and $i+1$. Let $T(x_i,t_j)$ and $u(x_i,t_j)$ be the tension and the displacement of the ith node, respectively, at time t_j. We neglect small variations in radius of curvature over the cable segment and denote it by $R(x_i)$. *It should be noted that such a standard discretization approximation is different from the assumption of constant curvature across the entire cable in the previous work [14]–[17] as one can always choose the discretization segment length* $\Delta \mathrm{x}_i$ *small enough to make the approximation error arbitrarily small in the proposed approach.* Without considering the segments, which are completely slacking (i.e., the segment of $u'(x,t) < 0$, which could happen at the two ends of the cable due to certain imposed boundary conditions) as they are not the normal working modes for cable actuated devices, all cable segments can be divided into three different categories as follows.

Case 1: The entire segment is moving. Since $\dot{u}\,(x,t) \neq\; 0$ for the cable segment $(x_i,x_{i+1}]$, the first case of (6) or, equivalently, (4) applies. Thus, noting the discretization approximation assumption that $R(x) = R(x_i)$ and $\mathrm{sign}\,(\dot{u}(x,t)) = \mathrm{sign}\,(\dot{u}(x_i,t))\;\; \forall x \in (x_i,\, x_{i+1}]$, one can integrate (4) over the segment as follows:

$$\int_{x_i}^{x} \frac{T'(x,t)}{T(x,t)}dx = \int_{x_i}^{x} \frac{\mu}{R(x_i)}\mathrm{sign}\,(\dot{u}(x_i,t))\,dx \qquad \forall x \in (x_i, x_{i+1}]\,. \quad (9)$$

On integrating over the segment $(x_i,x]$, we get

$$T\,(x,t) = T\,(x_i,t)\exp\left(\frac{\mu\,(x - x_i)}{R\,(x_i)}\mathrm{sign}\,(\dot{u}(x_i,t))\right). \quad (10)$$

From (5), with the tension distribution of (10) over the segment, the displacement or the stretch in the cable segment can be analytically calculated by

$$\int_{x_i}^{x} u'(x,t)dx = \frac{1}{K}\int_{x_i}^{x} T(x_i,t)\exp\left(\frac{\mu(x-x_i)}{R(x_i)}\mathrm{sign}(\dot{u}(x_i,t))\right)dx \quad (11)$$

which, upon integration, gives us the following equation:

$$u(x,t)-u(x_i,t)=\frac{R(x_i)}{K\mu}\mathrm{sign}(\dot{u}(x_i,t))\,T(x_i,t) \times\left[\exp\left(\frac{\mu(x-x_i)}{R(x_i)}\mathrm{sign}(\dot{u}(x_i,t))\right)-1\right]. \quad (12)$$

Therefore, at the discrete time instant t_j, from (10) and (12), tension and displacement of the two ends of the ith cable segment can be approximated as given by the following equations:

$$T_{i+1}^{j}=T_i^{j}\exp\left(\frac{\mu(x_{i+1}-x_i)}{R(x_i)}\mathcal{S}_i^{j}\right) \quad (13)$$

$$u_{i+1}^{j}-u_i^{j}=\mathcal{S}_i^{j}\frac{R(x_i)}{K\mu}T_i^{j}\left[\exp\left(\frac{\mu(x_{i+1}-x_i)}{R(x_i)}\mathcal{S}_i^{j}\right)-1\right] \quad (14)$$

where for compactness, the notation $T_i^j \triangleq T(x_i,t_j)$, $u_i^j \triangleq u(x_i,t_j)$, and $\mathcal{S}_i^j \triangleq \mathrm{sign}(u(x_i,t_j)-u(x_i,t_{j-1}))$ have been used.

Case 2: The entire cable segment is stationary. Since the cable segment is stationary, the strain of the segment will not change. Subsequently, the tension of the segment does not change either. Thus, displacement and tension of the two nodes remain unchanged from the previous values, i.e.,

$$T_i^j=T_i^{j-1} \text{ and } T_{i+1}^j=T_{i+1}^{j-1}$$
$$u_i^j=u_i^{j-1} \text{ and } u_{i+1}^j=u_{i+1}^{j-1}. \quad (15)$$

Case 3: A part of the cable segment is moving, while the rest of it is stationary. Without loss of generality, assume that node i is moving, while node $i+1$ is stationary. Let ξ be the last moving point on the cable segment, i.e., $\xi=\max\{x\in[x_i,x_{i+1}] \,:\, u(x,t_j)\neq u(x,t_{j-1})\}$. Therefore, Case 1 applies for the section $(x_i,\,\xi]$, while Case 2 for the rest of the segment. Thus, the tension and displacement remain unchanged over the section $(\xi,x_{i+1}]$, i.e.,

$$T(x,t_j)=T(x,t_{j-1}) \text{ and } u(x,t_j)=u(x,t_{j-1}) \quad \forall x\in(\xi,x_{i+1}]. \quad (16)$$

Since only node information is preserved in the discrete time model, the actual tension and displacement of $T(x,t_{j-1})$ and $u(x,t_{j-1})$ for the section $x\in(\xi,x_{i+1})$ in the previous time instance are lost at the current time instance. Thus, one cannot explicitly calculate the exact tension and displacement variation across the section (ξ,x_{i+1}), and some sorts of further approximations have to be made. Fortunately, since a small cable segment is assumed in the discretization process, we may approximate the strain over the segment by the strain calculated based on the average tension of the two ends of the cable segment, i.e., assuming $u'(x,t)\approx(1/K)((T_i^j+T_{i+1}^j)/2)$, $\forall x\in(x_i,x_{i+1}]$. With this approximation, the cable displacement over the segment can be calculated as follows:

$$u(x,t)-u_i^j=\frac{T_i^j+T_{i+1}^j}{2K}(x-x_i) \quad \forall x\in(x_i,x_{i+1}]. \quad (17)$$

Note that cable stretch, as calculated in (17), is accurate in case of constant tension across the segment. In the case of the entire segment being in motion as in Case 1, it represents a second-order approximation of the tension profile given by (12), which can be proven by noting $(e^y-1)/y=(1+e^y)/2+O(y^3)$. Combining (16) and (17), the tension and displacement transmissions over the segment are calculated by

$$u_{i+1}^j=u_{i+1}^{j-1}, \quad T_{i+1}^j=T_{i+1}^{j-1} \quad (18)$$

$$u_i^j=u_{i+1}^j-\frac{T_i^j+T_{i+1}^j}{2K}(x_{i+1}-x_i). \quad (19)$$

These three cases cover all the possible scenarios of motion during the normal operating conditions. The analysis has been carried out based on the system dynamics, making no assumption related to the discretization for all the moving nodes. Spatial discretization assumption is only made for the partially moving cable segment. Thus, its effects are minimal. Since no assumption has been made related to the temporal discretization, it does not directly affect the simulations. However, it affects the last moving point in the partially moving node and, thus, indirectly affects the accuracy of the simulations. Although no analysis has been presented here to determine the number of elements into which the cable should be divided, simulations can be used to find the optimal number of elements. We can now use these equations to simulate the motion and torque transmission characteristics of a cable-conduit system.

IV. Simulation Results

To simulate the motion and torque transmission, we start by defining conduit shape, initial condition, and boundary conditions, as discussed in (7) and (8). Although the initial pretension may not be constant across the entire cable in practice, in order to compare the proposed method with previous work, a constant pretension T_0 is assumed in the following simulations, which translates to the initial condition to

$$u'(x,0)=T_0/K \quad \text{or} \quad u(x,0)=T_0x/K+u(0,0). \quad (20)$$

The number of cable segments for simulations can be determined based on the accuracy levels desired, either by analysis or by iterations. With initial condition in (20) and boundary condition in (8), we simulate the system for required number of segments for each cable, assuming that the system starts from rest (or some pre-specified state). Because of the presence of friction, motion transmission is not instantaneous. Thus, all the segments do not start moving immediately when an input motion is applied. Therefore, at any time instant, for each cable segment, it is identified whether the segment is moving, partially moving, or stationary. Based on this information, the ''*last moving node*'' of the cable is estimated.

Consider the motion of cable A. For simplicity, we assume that at $t_0 = 0$, all the nodes are stationary. Without loss of generality, consider the case when the cable is being pulled at $x_1 = 0$ with an enforced boundary given by (8), as shown in Fig. 3. Therefore, at $t = t_1$, $\dot{u}(x_1, t) = \dot{g}_{id}(t) < 0$ and the motion starts propagating along the cable. By the time t_p, let node k be the "*last moving node*," i.e., the motion has been propagated over the segments from 1 to k – 1 but has not reached node k + 1. Thus, Case 1 in previous section applies to the first k–1 segments, Case 3 for the segment *k,* and Case 2 for the rest of the segments, which leads to the following set of equations:

$$\begin{aligned} T_1^p \exp\left[\frac{\mu \Delta x_1}{R(x_1)} \mathcal{S}_1^p\right] - T_2^p &= 0 \\ &\vdots \\ &\vdots \\ T_{k-1}^p \exp\left[\frac{\mu \Delta x_{k-1}}{R(x_k)} \mathcal{S}_{k-1}^p\right] - T_k^p &= 0 \quad \ldots k-1 \text{ eqns.} \end{aligned} \tag{21}$$

$$\begin{aligned} & u_2^p - \frac{R(x_1)}{K\mu} \mathcal{S}_1^p T_1^p \left[\exp\left(\frac{\mu \Delta x_1}{R(x_1)} \mathcal{S}_1^p\right) - 1\right] = g_{id}(t_p) \\ & u_3^p - u_2^p - \frac{R(x_2)}{K\mu} \mathcal{S}_2^p T_2^p \left[\exp\left(\frac{\mu \Delta x_2}{R(x_2)} \mathcal{S}_2^p\right) - 1\right] = 0 \\ & \vdots \\ & \vdots \\ & u_k^p - u_{k-1}^p - \frac{R(x_{k-1})}{K\mu} \mathcal{S}_k^p T_{k-1}^p \left[\exp\left(\frac{\mu \Delta x_{k-1}}{R(x_{k-1})} \mathcal{S}_k^p\right) - 1\right] = 0 \\ & u_k^p + \frac{T_k^p}{2} \frac{\Delta x_k}{K} = u_{k+1}^{p-1} - \frac{T_{k+1}^{p-1}}{2} \frac{\Delta x_k}{K} \quad \ldots k \text{ eqns.} \end{aligned} \tag{22}$$

With the boundary conditions imposed by the actuating motion of the end of the cable, $u(x_1, t_p) = g_i d(t_p)$, and stationary node $k+1$, $u(x_{k+1}, t_p) = u(x_{k+1}, t_p - 1)$, the motion of all the intermediate nodes $u(x_2, t_p)$, $u(x_2, t_p)$,. . ., $u(x_k, t_p)$ are unknown (k – 1 unknowns). In addition, tension of the first k nodes $T(x_1, t_p)$, $T(x_2, t_p)$, . . ., $T(x_k, t_p)$ are unknown (k unknowns), the tension of node $k + 1$ being known from previous time step. Therefore, these $2k$ – 1 unknown displacement and tension variables can be calculated by simultaneously solving the $2k$ – 1 equations in (21) and (22). The kth cable segment starts to move, and node k + 1 becomes the last moving node at time t_q when the following condition is satisfied:

$$T(x_{k+1}, t_{q-1}) \mathcal{S}_k^p \geq T(x_k, t_q) \mathcal{S}_k^p \exp\left[\frac{\mu \Delta x_k}{R(x_k)} \mathcal{S}_k^p\right]. \tag{23}$$

As the nodes at x_1 and x_{n+1} keep on moving, tension at the input ends keep on changing, and motion propagates along the two cables A and B. Eventually, the last moving nodes of both the cables coincide and the cables start to move *en masse*. Apart from computational perspective, the concept of last moving node also helps us in physically analyzing the partial motion transmission across the cable. This becomes particularly useful for understanding the coupled motion transmission in a two-cable system, where one cable starts pulling another cable, as elaborated upon later in this section. If, at any point in time, tension on one of the cables becomes zero (cable goes slack), e.g., cable B, only the nodes of the other cable, as well as the distal node of the slack cable (i.e., node 1, 2,. . . , n, $2n$ in this case), need to be solved for motion transmission.

Since the motion of two cables are constrained by the pulleys connecting them, assuming no slacking at the two pulleys

$$\begin{aligned} u(x_n, t) - u(x_{2n}, t) &= 2R_o\theta_o \\ u(x_n, t) + u(x_{2n}, t) &= 2L. \end{aligned} \tag{24}$$

Simulations are carried out assuming negligible friction losses at the pulleys as compared with the losses in the conduits. Thus, the boundary condition in (8) can be simplified as follows:

$$\tau_o = -K_e\theta_o = (T_2 - T_4)R_o \tag{25}$$

where τ_o is the external torque being applied by the load, θ_o is its angular rotation at the output, R_o is the radius of the pulley attached to the load motor, K_e is the simulated environment stiffness, $2L$ is the sum of two conduit lengths corresponding to cables A and B, and T_k (k = 1, 2, 3, 4) denote the tension at the two ends of each cable, i.e., $T_1(t) = T(x_1, t)$, $T_2(t) = T(x_n, t)$, $T_3(t) = T(x_{n+1}, t)$, and $T_4(t) = T(x_{2n}, t)$.

The input motor is simulated to follow a sinusoidal oscillatory motion profile. At each time step, based on the aforementioned discussion, the last moving node of each cable is estimated for the given input motion. The tension and displacements of all the nodes up to the last moving node are calculated accordingly. If one of the cables goes slack, the parameters for the other cable are calculated as an independent cable with the corresponding load, since the slack cable no longer affects its motion. Based on the earlier analysis, the motion of the system can be divided in two categories: 1) both cables taut or 2) either cable slack.

Simulations are carried out for the two-cable system, where each cable is of length 2 m, looped thrice, with a pretension of T_0 = 10 N; the equivalent stiffness of the cable-conduit system is 1 kN/m, and the environment stiffness is 0.4 kN·m. The cables are divided in 16 sections each, and a time step of 0.25 ms was used for the simulations. A sinusoidal motion of amplitude 1 rad and frequency of 1 Hz is applied as the input. Simulation results are shown in Fig. 5. Various time instants have been marked by numbers to facilitate the comparison of various parameters as well as correlating the trends in different plots. For simplicity, time instant 1 has been chosen when the direction of motion changes for the first time. The tension transmission across the two cables, i.e., cable A and cable B, is shown in Fig. 5(a) and (b), respectively. Although the tension transmission profiles are largely similar to the case of single cable transmission, differences due to cable coupling are visible as "peaks" in the transmission profile (highlighted by the dotted circle), which are discussed in detail later in the section as phase II (one cable pulling another cable). The overall tension profiles

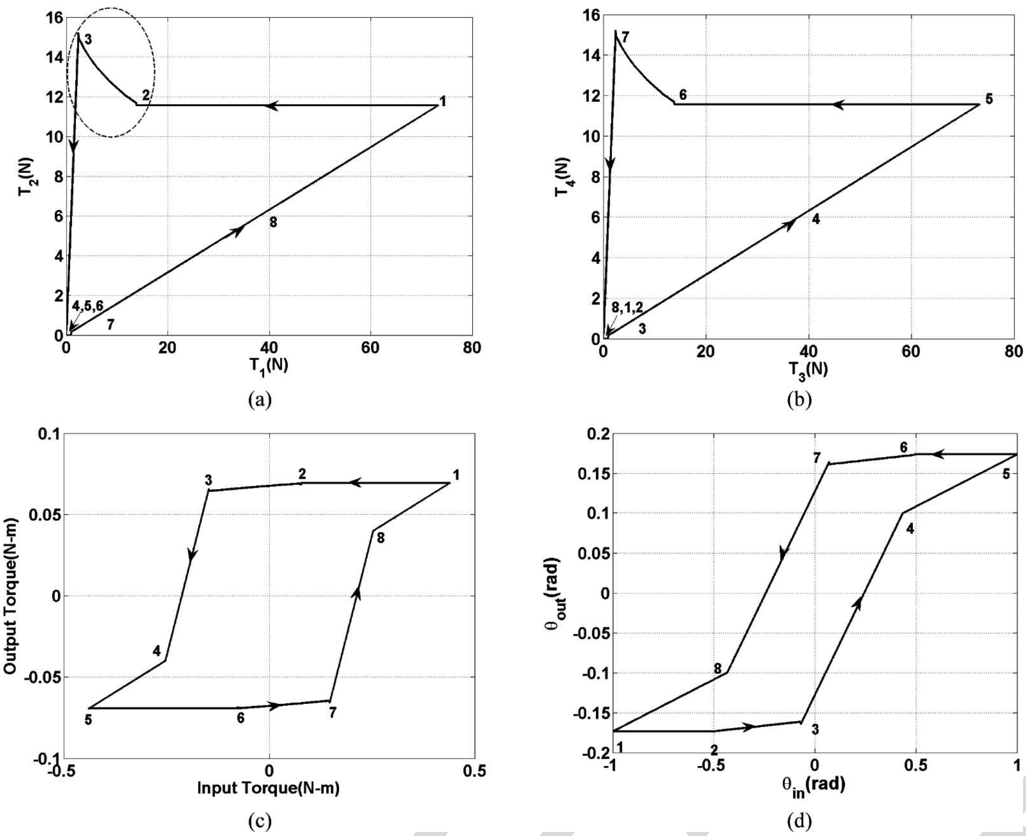

Fig. 5. *Transmission profile* with various time instants. (a) Tension transmission across cable A (T_1 versus T_2) and (b) across cable B (T_3 versus T_4). (c) Torque transmission from the actuator ($\tau_{\rm in}$) to the load ($\tau_{\rm out}$). (d) Angular rotation transmission from the drive pulley ($\theta_{\rm in}$) to the follower pulley ($\theta_{\rm out}$).

are similar for the two cables, as shown in Fig. 5(a) and (b), however, with different states at any time instant.

Apart from comparing the tension variation, in the case of the two-cable system, we can also compare torque and angular motion transmission from the actuator to the load. The torque transmission is shown in Fig. 5(c), and the angular motion propagation is shown in Fig. 5(d). Both the torque and motion transmission follow a backlash type of profile, however, with different slopes and widths.

To understand the mechanism of motion propagation across the cable, consider Fig. 6, showing the variation of output torque versus input torque ($\tau_{\rm in}$ versus $\tau_{\rm out}$). The transmission profile can be divided in various phases, as marked in the figure. These phases can be briefly described as follows.

1) *Output pulley not moving:* When the motion has not propagated to the distal end of either of the two cables (i.e., the output load), both the cables move independently, and as a result, no torque is transmitted to the output, and the output pulley does not move. This corresponds to the width of the backlash, as represented by the flat sections (time intervals 1–2 and 5–6 in Fig. 5).

2) *One cable pulling another cable:* Because of difference in tension across the two cables, friction levels are also different, and as a result, the rate of motion propagation varying across the two cables is also different. Therefore, there are time instances when motion propagates to the end of only one cable (without loss of generality assume cable A), while the other cable (cable B) is partially moving. Thus, cable A is causing the output pulley to move, as well as the distal end of cable B, while the (partial) motion of the drive end of cable B does not influence the motion of the load pulley. This gives rise to the section with small slope in the backlash profile (time intervals 2–3 and 6–7), since only one cable is active in motion transmission to the load, which is also referred to as soft spring [12]. In

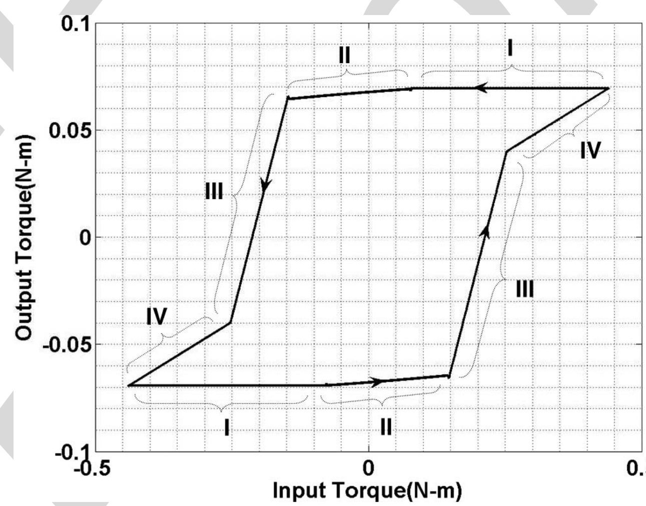

Fig. 6. Torque transmission profile.

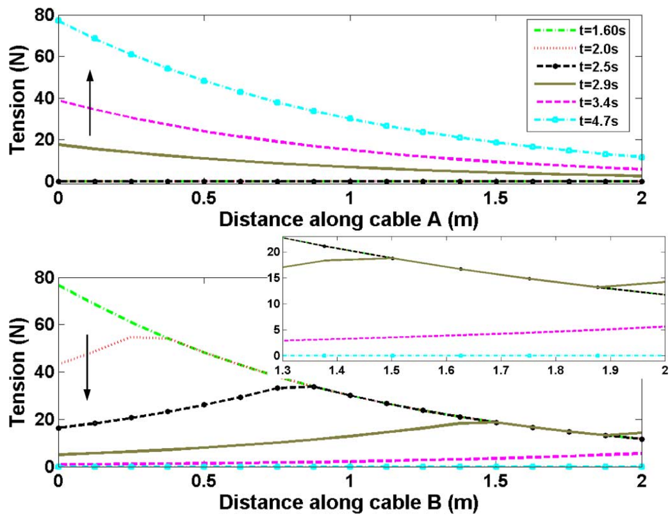

Fig. 7. Tension variation across the length of the two cables.

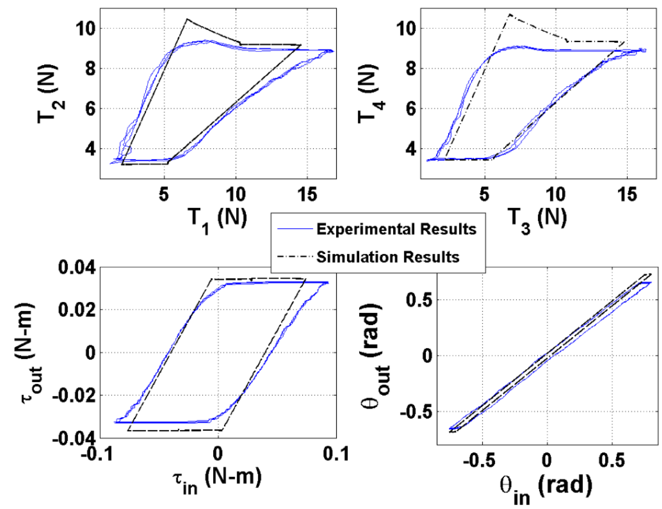

Fig. 8. Experimental and simulation results for $T_0 = 7.3$ N, using the original parameter estimates.

the tension transmission profile, this gives rise to the phase when (in cable B); although the tension at the drive end of the cable is decreasing, the tension at the follower end is increasing (due to pulling by cable A), as shown by the solid brown line in Fig. 7 and dotted circle in Fig. 5(a). Thus, the interaction between the two cables gives rise to these *counter-intuitive* peaks in tension transmission profile, which is not visible in the case of single cable.

3) *Both cables moving:* When the last moving nodes of both the cables coincide, both the cables collectively move, transmitting torque to the output, which corresponds to the slope of the backlash in the torque as well as motion transmission (time intervals 3–4 and 7–8).

4) *One cable slack, while other cable is moving:* Depending on the input motion profile and the pretension, large tension drop across one of the cable can lead to cable slacking, while the tension across the other cable increases, and it keeps moving. This decreases the slope of the backlash, since only one cable is effectively transmitting motion, and hence, the apparent stiffness of the system reduces (time intervals 8–1 and 4–5). This phase can be further subdivided into two cases: a) Motion of the drive pulley continues in the same direction, and b) drive pulley changes its direction of motion.

These four phases define the cable motion. While phases I and II are generally of short time duration, phases III and IV govern the motion during most of the operation. Note that the occurrence and strength of all these phases are dependent on cable pretension as well as the amplitude of the input motion, apart from physical parameters of the system like cable length, stiffness, friction level, and environmental stiffness. From these plots, it is evident that friction not only causes a backlash type of transmission profile but also leads to other phenomenon, such as changes in the slope of the transmission due to cable slacking, introduction of small slopes in the torque transmission, as well as opposite tension variations at two ends of the cable due to partial motion propagation.

V. Experimental Results

To validate our simulation, experiments were performed using the setup described in Section II. The actuation cables were 0.52 mm in diameter, uncoated stainless steel 7 × 19 wire rope that is approximately 1.6 m in length and wrapped around 12-mm-diameter motor pulleys. The stainless steel conduits were 1.2 m in length, made from 0.49-mm-diameter wire wrapped into a close-packed spring with an inner diameter of 1.29 mm. The two motors were controlled using the dSpace control board. For this study, the pretension in the cables and shape of the conduit could be varied and controlled. Pulley rotation was measured with a resolution of 0.18°. Pulley torque was measured with an accuracy of 0.1 mN·m over a range of 100 mN·m, while the combined cable tension measured by the load cell had an accuracy of 0.1 N over a range of 45 N.

To correlate the experimental results with the simulation, several system properties were experimentally estimated. In particular, the stiffness of the cable and conduits were measured to be 15.43 and 137.76 kN/m, respectively. Since the cable and the conduits act as springs in parallel, the equivalent cable stiffness was calculated to be 13.88 kN/m. Force relaxation or the creep of the cable was measured to be approximately 10.5%, with a time constant of approximately 30 s and, therefore, deemed negligible for these initial experiments. The friction coefficient between the cable and the conduit was measured to be 0.147, and the viscous friction was negligible and could be ignored as experimental error.

Fig. 8 shows the experimental and simulation results for a half loop in the conduit. The pretension in the experiments was approximately set at $T_0 = 7.3$ N, applying a uniform pretension across the cable not being possible due to the friction effects. The simulations capture all the major trends observed in experiments and match the numbers closely. In the experimental results, for the tension transmission profile, we observe a hump or a peak as predicted by the simulations. In addition, the

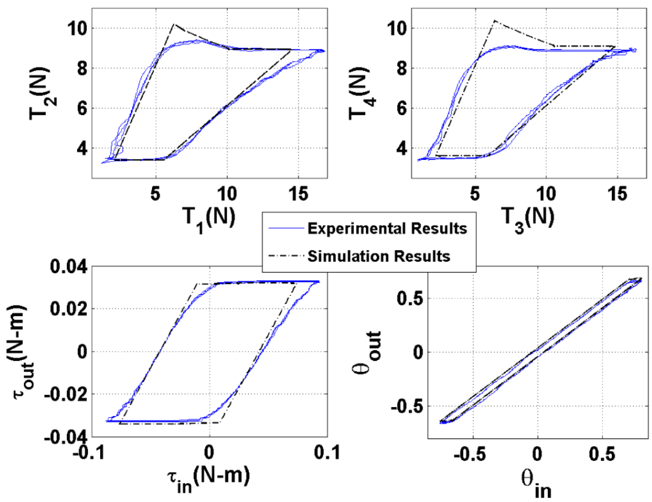

Fig. 9. Fitting of experimental results and simulation results for the recalculated cable parameter $k = 7.5$ kN/m, and $\mu = 0.156$.

TABLE I
NORMALIZED ERROR PERCENTAGE

	θout	*τ_in*	*τ_out*	T_1	T_2	T_3	T_3
R.M.S.E. (%)	3.7	19.4	3.7	12.8	4.1	9.9	5.5

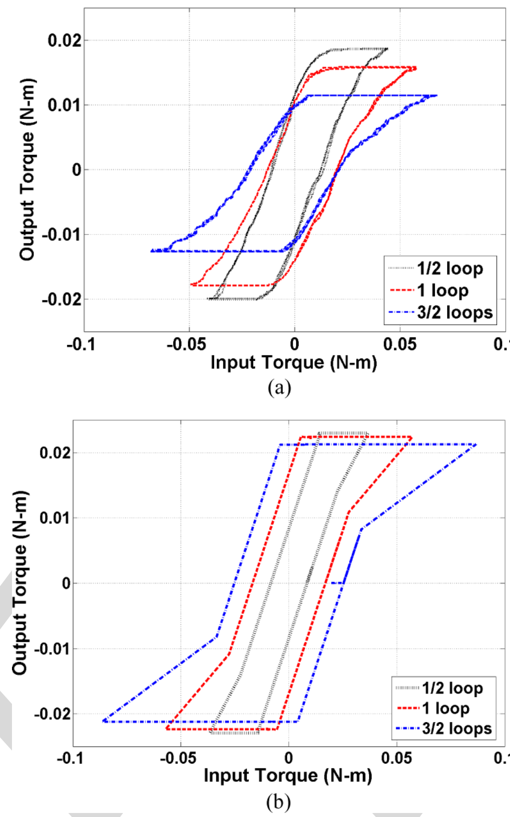

Fig. 10. Variation in torque transmission with number of loops. (a) Experimental results for different number of loops in conduit. (b) Simulation results for corresponding number of loops.

backlash in the torque and motion transmission is similar to what is predicted in the simulation results.

To analyze, goodness of fit between simulation and experimental results, the model was fitted on the experimental data to back calculate the cable stiffness and friction coefficients as 7.75 kN/m and 0.156, respectively. Using these parameters, the simulations were carried out again and compared with experimental results, as shown in Fig. 9. Table I shows the normalized rms percentage over one cycle for various parameters.

In the following sections, the effect of variation in cable pretension and conduit path has been studied, and the change of behavior as captured by simulations and experiments are compared.

A. Variation of Conduit Path

Friction is exponentially correlated to the angle of curvature of the conduit. Thus, increasing the curvature angle should increase the friction and, hence, larger backlash width. Larger friction also leads to longer time periods when one of the cables is slack, while the other cable is moving (phase IV), as well as smaller slope during this phase. To verify this, the curvature angle of the conduit is varied, while all the other parameters are kept constant, and its effect on the transmission profile is observed. For simplicity, the conduit shape was changed by adding additional ''*half-loops*'' or *180°* of bend. For introducing loops, the entire length of the conduits was used such that the radius of curvature remained constant throughout the conduit. To maintain uniformity in pretension, cables were loaded after changing the number of loops. The simulation results in Fig. 10(b) match well with the experimental results in Fig. 10(a). An increase in the backlash width, as well as change in the slope, as seen in experimental results, have been well predicted by the simulations.

B. Variation of Pretension

Since, according to (2), the tension loss is directly proportional to pretension, increasing the pretension increases the backlash. For a large pretension of 7 N, cables do not slack, and therefore, phase IV is not present. For a pretension of 3.5 N, phase IV is present, when one cable goes slack, while the other is still moving. This is also visible for the pretension of 0.7 N, but in this case, an additional trend is present, showing the second case of phase IV when one cable remains slack, while the other cable is moving, and the input switches its direction of motion. Experimental results in Fig. 11(a) show the change in the backlash width as well as cable slacking (both phase IVa and IVb), which can also be observed in simulation results in Fig. 11(b).

C. Variation of Loop Radius

According to (4), tension variation across the cable is related to $\Delta x/R \doteq \Delta\theta$. Therefore, for a constant angle of curvature $\Delta\theta$, the model predicts that there is no effect on system behavior with a change in the radius of curvature. To verify this, experiments were carried out for three different loop radii of 4.57, 6.35, and 7.62 cm (1.8, 2.5, and 3 in), while keeping the curvature angle

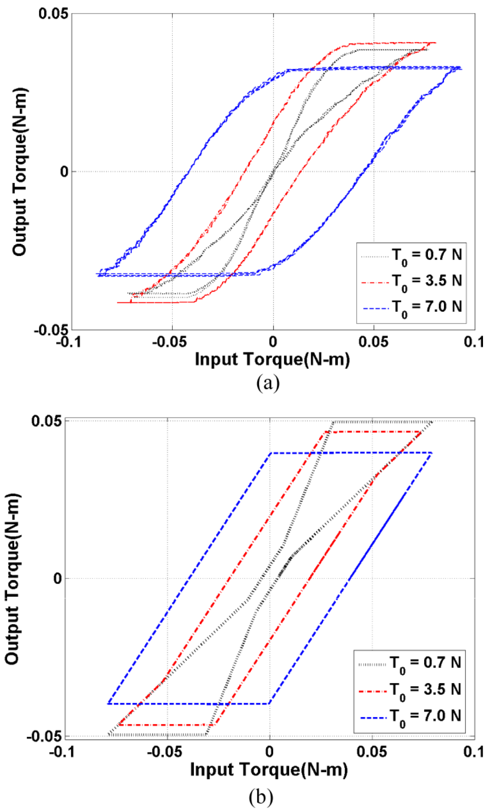

Fig. 11. Variation in torque transmission with pretension in the cables. (a) Experimental results for different cable pretension. (b) Simulation results for corresponding variation in pretension.

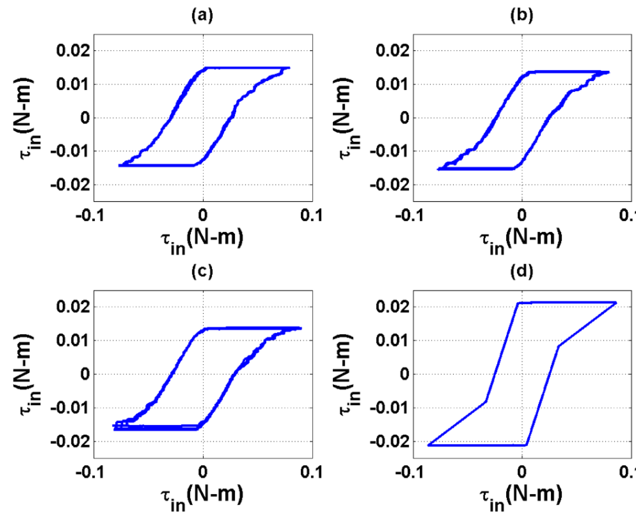

Fig. 12. Variation in torque transmission with loop radius. Experimental results for loop radius (a) 4.57 cm, (b) 5.35 cm, (c) 7.62 cm, and (d) corresponding simulation result.

same. Constant radius was implemented by wrapping the conduit around a circular object. Similar to Section V-A, pretension was applied after changing the number of loops. Corresponding experimental torque profiles are shown in Fig. 12(a)–(c), while the simulation result is shown in Fig. 12(d). From the plots, it can be inferred that the variation with the loop radius is minimal, as predicted by the model.

VI. Conclusion

Although using a pair of cables in pull–pull configuration provides simple and cost-effective power transmission in a surgical robot as well as other robotic devices, its use has been limited due to the nonlinearities generated due to friction and compliance present in the system. A system model was needed to analyze the nonlinearities in the system and to understand the tradeoffs involved arising from tension losses and cable slacking due to friction. While transmission models have been developed earlier, their application scope was quite restricted due to the assumptions of single-cable transmission, constant curvature, and cable pretension.

In this paper, starting from the system dynamics, we have developed a discretized model of the transmission characteristics of the system. The model has been validated on the experimental setup developed, which emulates a typical robot actuation. Simulations were successful not only in predicting the trends of the transmission characteristics in the experimental setup but in the magnitudes of various parameters with high accuracy as well. The differences in experimental and simulation results can be attributed to various approximations inherent in the system modeling, experimental errors, as well as errors in system parameter identification. Although due care was taken, kinks may have been inadvertently introduced in the cables, which also deteriorate the system performance.

For the modeling cable inertia that has been neglected, typical cable mass is less than 2 gm/m for the steel cables used. However, at extremely low-tension levels and inflection or singularity points in motion trajectory, inertia may not be negligible. The simulations use static Coulomb friction model. Using a dynamic friction model, like Dahl's friction model, may provide better results. The use of Coulomb friction model, together with negligible inertia, might be the reason of sharp transition in simulations, which are not present in the experimental results. The model also neglects the effects of force relaxation and friction effects at the two pulleys. Although placement of the loop along the conduit has not been explicitly discussed, the model captures its effects by appropriately defining the conduit curvature. Loop placement does not directly change the capstan effect; however, it changes the cable elongation and, therefore, also changes the overall transmission profile.

Although the environmental load has been assumed as a torsional spring, it can be conveniently modified for a generic load in (25). Although corresponding simulations have not been carried out, the results are expected to follow a similar friction dependent backlash-type behavior, since the deadband is dependent on friction due to cable pretension and not on the external load. For the experiments, a constant radius has been used. However, in practice, various sensors, e.g., fiber optic sensors can be placed along the conduit, which can be used to estimate the conduit curvature. The model can be further improved by incorporating the load dynamics. The current model assumes high-conduit bending stiffness and does not model the changes in pretension, which occur due to the changes in the path of conduit due to lateral forces exerted by the cable.

This system model, while reinforcing the results obtained in other publications, also bring up some key phenomena not observed earlier, particularly due to cable coupling. An attempt has been made to duly highlight all these aspects using the simulation results. Apart from torque transmission, motion transmission, which is necessary for position control, has also been presented, which was completely ignored in previous work. Furthermore, due analysis has been done to highlight all the physical parameters, as well as experimental conditions, which affect the motion transmission. Since the model has been validated, in the future, this model can be used to develop new control strategies for both force control as well as position control. An effective controller implementation can lead to active usage of cable drives in robotic systems, particularly in surgical robots, where the cable conduits can bring dexterity and flexibility in laparoscopic surgical robots, which the current systems lack.

REFERENCES

[1] V. Agrawal, W. J. Peine, and B. Yao, "Modeling of closed loop cable-conduit transmission system," in *Proc. IEEE Int. Conf. Robot. Autom.*, Pasadena, CA, May 2008, pp. 3407–3412.

[2] G. S. Guthart and J. K. Salisbury, "The intuitive telesurgery system: Overview and applications," in *Proc. IEEE Int. Conf. Robot. Autom.*, San Francisco, CA, Apr. 2000, pp. 618–621.

[3] R. J. Fanzino, "The Laprotek surgical system and the next generation of robotics," *Surg. Clin. N. Amer.*, vol. 83, no. 6, pp. 1317–1320, Dec. 2003.

[4] L. Biagiotti, F. Lotti, C. Melchiorri, G. Palli, P. Tiezzi, and G. Vassura, "Development of UB hand 3: Early results," in *Proc. IEEE Int. Conf. Robot. Autom.*, Barcelona, Spain, Apr. 2005, pp. 4488–4493.

[5] F. Lotti and G. Vassura, "A novel approach to mechanical design of articulated finger for robotic hands," in *Proc. IEEE/RSJ Int. Conf. Intell. Robots Syst.*, Lausanne, Switzerland, Oct. 2002, pp. 1687–1692.

[6] A. Nahvi, J. M. Hollerbach, Y. Xu, and I. W. Hunter, "Investigation of the transmission system of a tendon driven robot hand," in *Proc. IEEE Int. Conf. Intell. Robots Syst.*, Munich, Germany, Sep. 1994, vol. 1, pp. 202–208.

[7] I. Kassim, W. S. Ng, G. Feng, S. J. Phee, P. Dario, and C. A. Mosse, "Review of locomotion techniques for robotic colonoscopy," in *Proc. IEEE lnt. Conf. Robot. Autom.*, Taipei, Taiwan, Sep. 2003, pp. 1086–1091.

[8] S. J. Phee, W. S. Ng, I. M. Chen, F. Seow-Choen, and B. L. Davies, "Locomotion and steering aspects in automation of colonoscopy," *Eng. Med. Biol. Mag., IEEE*, vol. 16, no. 6, pp. 85–96, Nov./Dec. 1997.

[9] J. F. Veneman, R. Ekkelenkam, R. Kruidhof, F. C. T. van der Helm, and H. Van Der Kooij, "Design of a series elastic- and Bowden-cable-based Actuation system for use as torque actuator in exoskeleton-type robots," *Int. J. Robot. Res.*, vol. 25, no. 3, pp. 261–281, 2006.

[10] A. Schiele, P. Letier, R. van der Linde, and F. Van Der Helm, "Bowden Cable actuator for force-feedback exoskeletons," in *Proc. IEEE Int. Conf. Intell. Robot. Syst.*, Beijing, China, Oct. 2006, pp. 3599–3604.

[11] A. Schiele, "Performance difference of Bowden Cable relocated and non-relocated master actuators in virtual environment applications," in *Proc. IEEE Int. Conf. Intell. Robots Syst.*, Nice, France, Sep. 2008, pp. 3507–3512.

[12] M. Kaneko, W. Paetsch, and H. Tolle, "Input-dependent stability of joint torque control of tendon-driven robot hands," *IEEE Trans. Ind. Electron.*, vol. 39, no. 2, pp. 96–104, Apr. 1992.

[13] W. T. Townsend and J. K. Salisbury, Jr., "The effect of coulomb friction and stiction on force control," in *Proc. IEEE Int. Conf. Robot. Autom.*, Mar. 1987, vol. 4, pp. 883–889. **Q4**

[14] M. Kaneko, T. Yamashita, and K. Tanie, "Basic considerations on xtransmission characteristics for tendon drive robots," in *Proc. Int. Conf. Adv. Robot.*, 1991, vol. 1, pp. 827–832.

[15] M. Kaneko, M. Wada, H. Maekawa, and K. Tanie, "A new consideration on tendon tension control system of robot hands," in *Proc. IEEE Int. Conf. Robot. Autom.*, Sacramento, CA, 1991, vol. 2, pp. 1028–1033.

[16] G. Palli and C. Melchiorri, "Model and control of tendon-sheath transmission systems," in *Proc. IEEE Int. Conf. Robot. Autom.*, 2006, pp. 988–993. **Q5**

[17] G. Palli and C. Melchiorri, "Optimal control of tendon-sheath transmission systems," in *Proc. IFAC Symp. Robot Control*, 2006.

Authors' photographs and biographies not available at the time of publication.

QUERIES

Q1: Author: Please check the IEEE membership information of the authors as the membership of the first two authors was mentioned only in the transmittal PDF and not in the original manuscript.

Q2: Author: Please check and confirm footnote first as typeset.

Q3. Author: Please spell out ‘PTFE’ in full, if possible.

Q4. Author: Please check Ref. [14] as typeset.

Q5. Author: Please provide page range for Ref. [17].

Modeling of Transmission Characteristics Across a Cable-Conduit System

Varun Agrawal, *Student Member, IEEE*, William J. Peine, *Member, IEEE*, and Bin Yao, *Senior Member, IEEE*

***Abstract*—Many robotic systems, like surgical robots, robotic hands, and exoskeleton robots, use cable passing through conduits to actuate remote instruments. Cable actuation simplifies the design and allows the actuator to be located at a convenient location, away from the end effector. However, nonlinear frictions between the cable and the conduit account for major losses in tension transmission across the cable, and a model is needed to characterize their effects in order to analyze and compensate for them. Although some models have been proposed in the literature, they are lumped parameter based and restricted to the very special case of a single cable with constant conduit curvature and constant pretension across the cable only. This paper proposes a mathematically rigorous distributed parameter model for cable-conduit actuation with any curvature and initial tension profile across the cable. The model, which is described by a set of partial differential equations in the continuous time-domain, is also discretized for the effective numerical simulation of the cable motion and tension transmission across the cable. Unlike the existing lumped-parameter-based models, the resultant discretized model enables one to accurately simulate the partial-moving/partial-sticking cable motion of the cable-conduit actuation with any curvature and initial tension profile. The model is further extended to cable-conduit actuation in pull–pull configuration using a pair of cables. Various simulations results are presented to reveal the unique phenomena like backlash, cable slacking, the interaction between the two cables, and other nonlinear behaviors associated with the cable conduits in pull–pull configuration. These results are verified by experiments using two dc motors coupled with a cable-conduit pair. The experimental setup has been prepared to emulate a typical cable-actuated robotic system. Experimental results are compared with the simulations and various implications are discussed.**

***Index Terms*—Cable-conduit actuation, cable compliance, friction, pull–pull configuration, surgical robot.**

I. Introduction

Surgical robots often utilize cable-conduit pairs in a pull–pull configuration to actuate the patient-side manipulators and slave instruments [2], [3]. Cable transmissions are preferred because they can provide adequate power through narrow tortuous pathways and allow the actuators to be located safely away from the patient. Cables are light weight and cost effective and greatly simplify the transmission. Cable-conduit actuation, which is also sometimes known as tendon sheath, or Bowden cable actuation, is also used in many robotic hands [4]–[6], as well as colonoscopy devices [7], [8]. To develop power dense yet ergonomic actuation for wearable interfaces, cable actuation is also used in exoskeleton robots [9]–[11]. The control of these systems, however, is challenging due to cable compliance and friction within the conduit. These nonlinearities introduce significant tension losses across the cable and give rise to motion backlash, cable slack, and input-dependent stability of the servo system [12], [13]. In the absence of a transmission model for the cable-conduit system, these nonlinear behaviors are not accounted for [9]–[11], leading to poor system performance. Although various physical measures are adopted including using PTFE-coated steel cables sliding in *slightly preloaded* Kevlar-reinforced housings [10] and keeping the cable-wrapping angles and pretension to low levels, they can only improve the system performance to a certain degree. Beyond that, one has to rely on effective control algorithms to improve the performance, which stresses the importance of developing a model for the transmission characteristics. This paper develops a model for the transmission characteristics in cable-conduit mechanisms to effectively analyze such a system.

Kaneko *et al*. [12] performed experiments on torque transmission from the actuator to the finger joint using a pair of cables passing through conduits. However, no analytical model was developed. These experiments assumed a large value of pretension in the cable to avoid any slacking. Since friction forces are directly dependent on cable pretension, it leads to a tradeoff between tension losses and cable slacking. Thus, cable slacking is an important phenomenon that should be addressed. Later on, the authors developed a model for a single cable passing through the conduit of fixed constant curvature with a given constant pretension throughout the cable [14], [15]. Based on the model, they analytically calculated the equivalent cable stiffness for a single cable. Furthermore, the authors proposed a lumped-mass numerical model for tension transmission across the cable. Through their model, they demonstrated the cable-conduit system display direction-dependent behavior and, hence, cannot be treated as a simple spring. However, their model essentially assumes that all points on the cable have the same initial pretension of a constant value and, as such, cannot consider the general behavior of a cable-conduit transmission, where the initial tension depends on the spatial positions. The calculation of last moving point when using multiple-lumped elements also assumes the same constant pretension across all elements, which essentially

Manuscript received December 10, 2009; revised April 27, 2010; accepted July 28, 2010. This paper was recommended for publication by Associate Editor A. Albu-Schäffer and Editor W. K. Chung upon evaluation of the reviewers' comments. This work ~~was supported~~ by Meere Company, South Korea. This paper was presented in part at the IEEE International Conference on Robotics and Automation, Pasadena, CA, 2008 [1].

The authors are with the School of Mechanical Engineering, Purdue University, West Lafayette, IN 47906 USA (e-mail: vagrawal@purdue.edu, peine@purdue.edu, byao@purdue.edu).

Color versions of one or more of the figures in this paper are available online at http://ieeexplore.ieee.org.

Digital Object Identifier 10.1109/TRO.2010.2064014

ignores the spatial dependence of the tension transmission across the cable and prevents accurate study of some of the unique phenomena associated with the cable-conduit actuation mechanisms, such as partial moving/partial sticking. In practice, due to the presence of friction, the residual tension or initial tension profile depends on the time history of past applied forces and cannot be assumed to be uniform across the cable. Moreover, in many applications, like surgical robots and exoskeletons, the conduit curvatures are path dependent, and thus, the model cannot be applied directly for these applications. Because of these issues, the assumption of constant curvature and a predetermined constant pretension across the entire cable severely limits the usefulness of the model. Palli and Melchiorri [16], [17] further refined the model using a dynamic Dahl's friction model instead of the simple Coulomb friction model but made the same assumptions of constant pretension and curvature for the lumped-element models. Furthermore, all these existing models only focus on power transmission using a single cable conduit and, therefore, cannot address the unique phenomena of cable slacking and cable interaction associated with the systems using a pair of cables for power transmission, like the ones studied in this paper.

Instead of using the lumped-mass analysis, this paper first develops an exact, continuous time-domain model described by a set of partial differential equations (PDE's), which is applicable to cable-conduit systems with any pretension and curvature profiles. In addition, this paper considers the complex interaction between a pair of cables in pull–pull. The exact infinite-dimensional model is then discretized to generate effective numerical simulation algorithms for motion and power transmissions. This can be used to solve the nonlinear system response to predict cable slacking and overall transmission characteristics of the system. The model is validated through experiments.

Unlike the single-cable system discussed in detail in the earlier research, the use of pair of cables induces cable interaction leading to behavior that is completely absent in the prior cases. While the previous models have been developed using lumped-mass analysis with inertia, our work uses the exact distributed system dynamics to generate the discretized model for analysis and simulation, although the cable inertia is neglected. Furthermore, the phenomenon of partial cable segment, which causes the cable interaction, can be explained. The approximation errors in the discretization process have been clearly laid out as well. Moreover, while only force transmission has been analyzed in previous research, motion transmission has also been presented here, which is particularly important for surgical devices, which are usually operated in position control mode. In the following sections, the setup of the problem is discussed followed by details of the proposed model and the simulation results. The methodology of experiments is outlined, and experimental results are presented and compared with the simulation results.

II. Motivation and Experimental Setup

In cable-drive robots, the slave manipulators are mechanically actuated using cable drives passing through a thin tube or conduit. Nonlinearities are introduced in motion transmission due to the friction forces between the cable and the conduit. Moreover, tension losses across the cable necessitate much higher actuating forces for relatively small loads. While high pretension is desired to avoid cable slacking, it comes with a drawback of higher friction forces. However, lower pretension leads to cable slacking. Thus, a tradeoff is required between cable slacking and large actuation forces. Since it is difficult to place sensors at the distal ends of the highly miniaturized instrument, such as in a surgical robot, the position and applied forces of the tool tip are difficult to estimate and control. Hence, the resultant accuracy of the system is extremely poor, as compared with industrial robots. In surgical robots, this results in continuous adjustment of the actuating input by the human in the loop, thereby potentially affecting the performance of the surgeon. The objective of this research is to model cable actuation in such a system and characterize the force and motion transmission from the actuator to the load. Ultimately, these models can be used to improve the control strategy of the system.

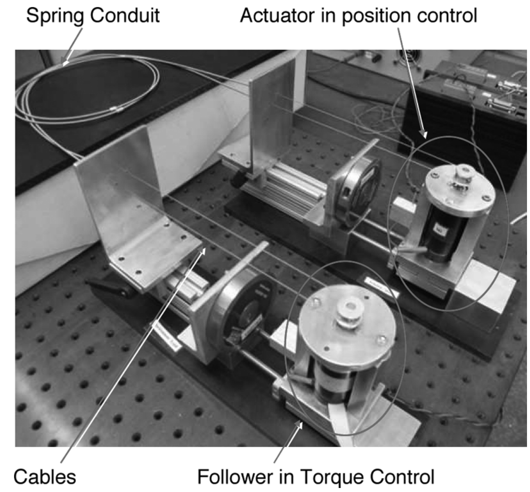

Fig. 1. Experimental setup.

A typical load actuation system of a cable actuated robot has been emulated in the experimental setup shown in Fig. 1. A schematic of the setup is shown in Fig. 2. A two-cable pull–pull transmission is used, actuated with two brushed dc motors mounted on linear slides. The first motor is controlled as the input or the drive motor, while the second motor simulates a passive load or environment. Each cable passes through a flexible conduit and is wrapped around pulleys attached to each of the dc motors. The tightly wound spring wire conduits are fixed at each end using two plates attached to the same platforms on which the linear slides are mounted. This way, the platforms holding the plates are free to move in space, and applying a tension in the cable is counteracted by a compression in the conduit with no forces being transmitted through the ground. The cable and the conduit, therefore, act as springs in parallel.

The actuator or the drive motor is run in position control mode, while the follower motor is run in torque control mode. The load is simulated as a torsional spring such that the restoring torque applied by the motor is proportional to the angle of rotation.

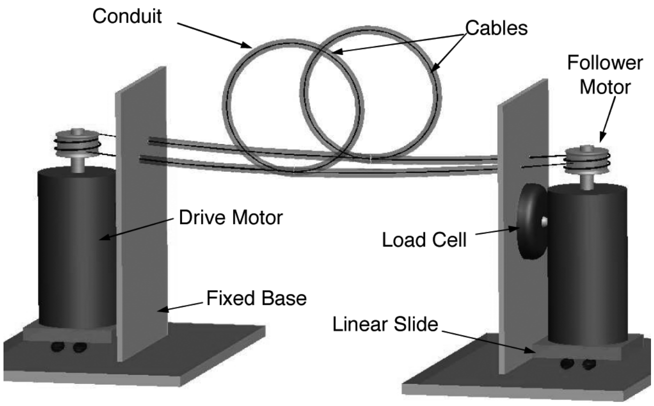

Fig. 2. Model of the experimental setup.

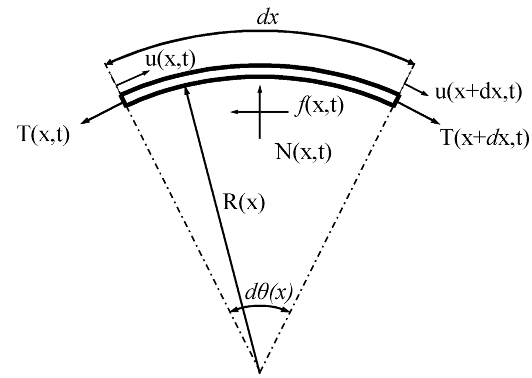

Fig. 4. Forces balance diagram of cable element.

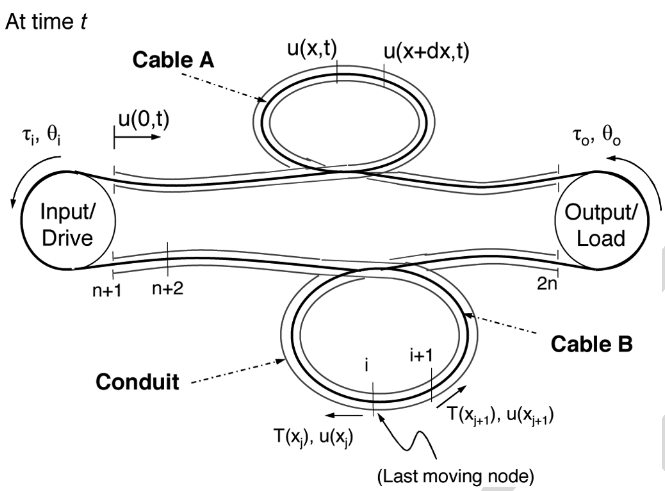

Fig. 3. Motion of the cable element.

Encoders are used to measure the angular rotation of the two motors. The current flowing across the two motors is used to estimate the torque applied by the pulley, which is proportional to the difference in the two cable tensions on each side. The sum of the tensions being applied by the two cables on each motor is measured using load cells mounted between the linear slide and conduit-termination plate. Using the torque values and the load cell measurements, tension at the two ends of each cable can be calculated.

III. Dynamic Model

A. System Governing Equations

Consider the setup shown in Fig. 3, where two flexible cables, i.e., cable A and cable B, pass through fixed conduits of predefined curvature $R(x)$, where x denotes the position along the conduit. At $t = 0$, actuator starts to move the cables. To model the motion of the cable, we make the following assumptions.

1) Inertia effects in the cable can be neglected.
2) The cable is restricted to move along conduit (no transverse motion).
3) Interaction between the cable and the conduit is through a normal force and friction (Coulomb friction).
4) Constitutive behavior of the cable is assumed to be elastic, defined by the standard Hooke's law.

When at relaxing state (i.e., no tension) without slacking, points on the cable can be uniquely indexed by the conduit position x. For the point on the cable indexed by x, let $u(x,t)$ denote its axial displacement at time t, and let $T(x,t)$ be the corresponding axial tension of the cable. For notational simplicity, in the following, the partial derivative of a function $T(x,t)$ with respect to the spatial variable x will be denoted by $T'(x,t)$ and the partial derivative with respect to the time variable t by $\dot{T}(x,t)$.

To obtain the dynamic model of the motion and force transmitted through the cable, consider the movement of an infinitesimal cable segment $[x,\ x + dx]$, as shown in cable A of Fig. 3 with an enlarged view shown in Fig. 4. In Fig. 4, $N(x,t)$ denote the normal force between the cable and the conduit. $f(x,t)$ is the frictional force acting on the cable. For this infinitesimal segment, the radius of curvature can be assumed to be constant, given by $R(x)$, and the infinitesimal angle $d\theta\,(x)$ shown in Fig. 4 is related to dx by $dx = R(x)d\theta(x)$. As there is no cable movement along the radial direction of the conduit, through the force balancing equation, the normal reaction force acting on this infinitesimal cable element is related to the tensions at the two ends by

$$\begin{aligned} N(x,t) &= T(x,t)\sin\left(\frac{d\theta(x)}{2}\right) + T(x+dx,t)\sin\left(\frac{d\theta(x)}{2}\right) \\ &\approx T(x,t)d\theta(x). \end{aligned} \tag{1}$$

Thus, from the Coulomb friction model, we know that

$$|f\,(x,t)|\ \le\ \mu N\,(x,t) =\ \mu T\,(x,t)\,d\theta\,(x) = \mu T\,(x,t)\,\frac{dx}{R\,(x)}. \tag{2}$$

As the inertia of the cable is neglected, the force balance equation applies to the axial direction of the conduit (i.e., the cable movement direction) as well. Therefore, when the net axial tension force $T(x{+}dx,t) - T(x,t) = T'(x,t)dx$ is less than the right-hand side of (2), i.e., $|T'(x,t)| < \mu T(x,t)/R(x)$, the cable segment will not move, and the actual friction $f(x,t)$ has the same magnitude as the net axial tension force, i.e.,

$$\dot{u}(x,t) = 0 \quad \text{and} \quad f(x,t) = T'(x,t)dx. \tag{3}$$

On the other hand, when the cable segment moves due to the net axial tension forces, friction will be at its maximum value, as given by (2), i.e., $f(x,t) = (\mu T(x,t)/R(x))\text{sign}\,(\dot{u}(x,t))\,dx$. Thus, from the force balance equation

$$T'(x,t)dx \;=\; \frac{\mu T(x,t)}{R(x)\text{sign}}\,(\dot{u}(x,t))\,dx \qquad \text{when } \;\dot{u} \neq 0. \quad (4)$$

To calculate the cable strain along the conduit path $u'(x,t)$, it is assumed that, when stretching, Hooke's law of elasticity can be used by modeling the cable as a linear spring with stiffness *K*, and when compressing or cable slacking, no force transmitted through the cable. Since the cable and the conduit act in parallel, K is the combined stiffness of the system. Thus

$$\begin{aligned} &T(x,t) = K\,u'(x,t) \quad \text{when} \quad u'(x,t) > 0\\ &T(x,t) = 0 \quad \text{when} \quad u'(x,t) \le 0\\ &\text{where} \quad \frac{1}{K} = \frac{1}{K_{\text{cable}}} + \frac{1}{K_{\text{conduit}}}. \end{aligned} \quad (5)$$

Combing (3)–(5), the overall distributed dynamic model of the motion and tension across the cable is described by the following sets of PDEs:

$$\begin{aligned} &\text{when} \;\; u'(x,t) > 0, \;\; T(x,t) = K\,u'(x,t) \text{ and}\\ &\quad \text{i)} \quad u''(x,t) - \frac{\mu}{R(x)}u'(x,t)\text{sign}\,(\dot{u}(x,t)) = 0\\ &\qquad\qquad \text{if } |u''(x,t)| = \frac{\mu}{R(x)}u'(x,t)\\ &\quad \text{ii)} \quad \dot{u}(x,t) = \;0, \qquad \text{otherwise}\\ &\text{when} \;\; u'(x,t) \le 0\\ &\quad \text{iii)} \quad T(x,t) = 0. \end{aligned} \quad (6)$$

Aside from the aforementioned governing equations, to calculate the motion and tension transmission across the cable, one needs the initial conditions and the boundary conditions as well. Thus, to be able to precisely describe the cable dynamic behavior, it is absolutely necessary to specify the initial cable displacement profile $u_0(x)$, i.e.,

$$u(x,0) = u_0(x) \quad (7)$$

and the boundary conditions of the cable at the two ends, depending on the environment to which the cable is attached. For example, consider a cable with the end at $x = 0$ connected to an environment having a predefined movement of $g_{id}(t)$ and the other end at $x = L$ fixed to a stiff environment having a stiffness of K_e; then, noting (7), the boundary conditions for solving the cable movement would be

$$\begin{aligned} &u\,(0,t) = g_{id}\,(t)\\ &u\,(L,t) = -\frac{1}{K_e}T\,(L,t) = -\frac{K}{K_e}\,u'(L,t). \end{aligned} \quad (8)$$

Remark 1: In the earlier development of the mathematically rigorous distributed parameter model for cable-conduit actuation, no restriction is put on the curvature of the conduit, i.e., $R(x)$ could be any function. This is in contrast with the previous work in [14]–[17], where constant curvature is assumed across each cable segment. Furthermore, no restriction is put on the initial cable displacement profile $u_0(x)$, and thus, the initial tension profile of $T\,(x,0) = K\,u'\,(x,0) = K\,u_0'\,(x)$ (assume that $u_0'\,(x) \ge 0$). *It is noted that all the previous work [14]–[17] assume a constant initial tension profile of* $T\,(x,0) = T_0$, *which is hardly true in reality due to the distributed friction effect across the cable.* Thus, although some of the discretized equations on the tension transmission for a particular segment introduced in the following section may look somewhat similar to those in [14]–[17], the overall modeling process is fundamentally different from the previous work. In addition, cable slacking is explicitly taken into account in the proposed model, which cannot be addressed using previous work.

B. Discretized Model

Since it is impossible to analytically solve the PDEs (6), in practice, discretized element models based on these governing equations are obtained for realistic computer simulations, which is the subject of this section. As shown by cable B in Fig. 3, the each cable is divided into n cable segments, with nodes at $x_1 = 0$, $x_2 = \Delta x_1$, $x_3 = x_2 + \Delta x_2, \ldots$, and $x_n = x_{n-1} + \Delta x_n = \sum_{i=1}^{n} \Delta x_i = L$. The displacement and tension of the two ends of each segment will be calculated at discrete time instants using the discretized elemental equations as follows.

Consider the ith cable segment between nodes i and $i + 1$. Let $T(x_i,t_j)$ and $u(x_i,t_j)$ be the tension and the displacement of the ith node, respectively, at time t_j. We neglect small variations in radius of curvature over the cable segment and denote it by $R(x_i)$. *It should be noted that such a standard discretization approximation is different from the assumption of constant curvature across the entire cable in the previous work [14]–[17] as one can always choose the discretization segment length* $\Delta \mathrm{x}_i$ *small enough to make the approximation error arbitrarily small in the proposed approach*. Without considering the segments, which are completely slacking (i.e., the segment of $u'(x,t) < 0$, which could happen at the two ends of the cable due to certain imposed boundary conditions) as they are not the normal working modes for cable actuated devices, all cable segments can be divided into three different categories as follows.

Case 1: The entire segment is moving. Since $\dot{u}\,(x,t) \neq \;0$ for the cable segment $(x_i,x_{i+1}]$, the first case of (6) or, equivalently, (4) applies. Thus, noting the discretization approximation assumption that $R(x) = R(x_i)$ and $\text{sign}\,(\dot{u}(x,t)) = \text{sign}\,(\dot{u}(x_i,t))\;\; \forall x \in (x_i,\, x_{i+1}]$, one can integrate (4) over the segment as follows:

$$\int_{x_i}^{x} \frac{T'(x,t)}{T(x,t)}dx = \int_{x_i}^{x} \frac{\mu}{R(x_i)}\text{sign}\,(\dot{u}(x_i,t))\,dx \qquad \forall x \in (x_i, x_{i+1}]\,. \quad (9)$$

On integrating over the segment $(x_i,x]$, we get

$$T\,(x,t) = T\,(x_i,t)\exp\left(\frac{\mu\,(x - x_i)}{R\,(x_i)}\text{sign}\,(\dot{u}(x_i,t))\right). \quad (10)$$

From (5), with the tension distribution of (10) over the segment, the displacement or the stretch in the cable segment can be analytically calculated by

$$\int_{x_i}^{x} u'(x,t)dx = \frac{1}{K}\int_{x_i}^{x} T(x_i,t)\exp\left(\frac{\mu(x-x_i)}{R(x_i)}\operatorname{sign}(\dot u(x_i,t))\right)dx \quad (11)$$

which, upon integration, gives us the following equation:

$$u(x,t)-u(x_i,t)=\frac{R(x_i)}{K\mu}\operatorname{sign}(\dot u(x_i,t))\,T(x_i,t) \times\left[\exp\left(\frac{\mu(x-x_i)}{R(x_i)}\operatorname{sign}(\dot u(x_i,t))\right)-1\right]. \quad (12)$$

Therefore, at the discrete time instant t_j, from (10) and (12), tension and displacement of the two ends of the ith cable segment can be approximated as given by the following equations:

$$T_{i+1}^j = T_i^j \exp\left(\frac{\mu(x_{i+1}-x_i)}{R(x_i)}\mathcal{S}_i^j\right) \quad (13)$$

$$u_{i+1}^j - u_i^j = \mathcal{S}_i^j\frac{R(x_i)}{K\mu}T_i^j\left[\exp\left(\frac{\mu(x_{i+1}-x_i)}{R(x_i)}\mathcal{S}_i^j\right)-1\right] \quad (14)$$

where for compactness, the notation $T_i^j \triangleq T(x_i,t_j)$, $u_i^j \triangleq u(x_i,t_j)$, and $\mathcal{S}_i^j \triangleq \operatorname{sign}(u(x_i,t_j)-u(x_i,t_{j-1}))$ have been used.

Case 2: The entire cable segment is stationary. Since the cable segment is stationary, the strain of the segment will not change. Subsequently, the tension of the segment does not change either. Thus, displacement and tension of the two nodes remain unchanged from the previous values, i.e.,

$$T_i^j = T_i^{j-1} \text{ and } T_{i+1}^j = T_{i+1}^{j-1}$$
$$u_i^j = u_i^{j-1} \text{ and } u_{i+1}^j = u_{i+1}^{j-1}. \quad (15)$$

Case 3: A part of the cable segment is moving, while the rest of it is stationary. Without loss of generality, assume that node i is moving, while node $i+1$ is stationary. Let ξ be the last moving point on the cable segment, i.e., $\xi = \max\{x \in [x_i, x_{i+1}] \;:\; u(x,t_j) \neq u(x,t_{j-1})\}$. Therefore, Case 1 applies for the section $(x_i, \xi]$, while Case 2 for the rest of the segment. Thus, the tension and displacement remain unchanged over the section $(\xi, x_{i+1}]$, i.e.,

$$T(x,t_j)=T(x,t_{j-1}) \text{ and } u(x,t_j)=u(x,t_{j-1}) \quad \forall x \in (\xi, x_{i+1}]. \quad (16)$$

Since only node information is preserved in the discrete time model, the actual tension and displacement of $T(x,t_{j-1})$ and $u(x,t_{j-1})$ for the section $x \in (\xi, x_{i+1})$ in the previous time instance are lost at the current time instance. Thus, one cannot explicitly calculate the exact tension and displacement variation across the section (ξ, x_{i+1}), and some sorts of further approximations have to be made. Fortunately, since a small cable segment is assumed in the discretization process, we may approximate the strain over the segment by the strain calculated based on the average tension of the two ends of the cable segment, i.e., assuming $u'(x,t) \approx (1/K)((T_i^j + T_{i+1}^j)/2)$, $\forall x \in (x_i, x_{i+1}]$. With this approximation, the cable displacement over the segment can be calculated as follows:

$$u(x,t)-u_i^j = \frac{T_i^j + T_{i+1}^j}{2K}(x-x_i) \quad \forall x \in (x_i, x_{i+1}]. \quad (17)$$

Note that cable stretch, as calculated in (17), is accurate in case of constant tension across the segment. In the case of the entire segment being in motion as in Case 1, it represents a second-order approximation of the tension profile given by (12), which can be proven by noting $(e^y - 1)/y = (1+e^y)/2 + O(y^3)$. Combining (16) and (17), the tension and displacement transmissions over the segment are calculated by

$$u_{i+1}^j = u_{i+1}^{j-1}, \quad T_{i+1}^j = T_{i+1}^{j-1} \quad (18)$$

$$u_i^j = u_{i+1}^j - \frac{T_i^j + T_{i+1}^j}{2K}(x_{i+1}-x_i). \quad (19)$$

These three cases cover all the possible scenarios of motion during the normal operating conditions. The analysis has been carried out based on the system dynamics, making no assumption related to the discretization for all the moving nodes. Spatial discretization assumption is only made for the partially moving cable segment. Thus, its effects are minimal. Since no assumption has been made related to the temporal discretization, it does not directly affect the simulations. However, it affects the last moving point in the partially moving node and, thus, indirectly affects the accuracy of the simulations. Although no analysis has been presented here to determine the number of elements into which the cable should be divided, simulations can be used to find the optimal number of elements. We can now use these equations to simulate the motion and torque transmission characteristics of a cable-conduit system.

IV. Simulation Results

To simulate the motion and torque transmission, we start by defining conduit shape, initial condition, and boundary conditions, as discussed in (7) and (8). Although the initial pretension may not be constant across the entire cable in practice, in order to compare the proposed method with previous work, a constant pretension T_0 is assumed in the following simulations, which translates to the initial condition to

$$u'(x,0)=T_0/K \quad \text{or} \quad u(x,0)=T_0x/K+u(0,0). \quad (20)$$

The number of cable segments for simulations can be determined based on the accuracy levels desired, either by analysis or by iterations. With initial condition in (20) and boundary condition in (8), we simulate the system for required number of segments for each cable, assuming that the system starts from rest (or some pre-specified state). Because of the presence of friction, motion transmission is not instantaneous. Thus, all the segments do not start moving immediately when an input motion is applied. Therefore, at any time instant, for each cable segment, it is identified whether the segment is moving, partially moving, or stationary. Based on this information, the ''*last moving node*'' of the cable is estimated.

Consider the motion of cable A. For simplicity, we assume that at $t_0 = 0$, all the nodes are stationary. Without loss of generality, consider the case when the cable is being pulled at $x_1 = 0$ with an enforced boundary given by (8), as shown in Fig. 3. Therefore, at $t = t_1$, $\dot{u}(x_1, t) = \dot{g}_{id}(t) < 0$ and the motion starts propagating along the cable. By the time t_p, let node k be the ''*last moving node*,'' i.e., the motion has been propagated over the segments from 1 to k – 1 but has not reached node k + 1. Thus, Case 1 in previous section applies to the first k–1 segments, Case 3 for the segment k, and Case 2 for the rest of the segments, which leads to the following set of equations:

$$\begin{aligned} T_1^p \exp\left[\frac{\mu\Delta x_1}{R(x_1)}\mathcal{S}_1^p\right] - T_2^p &= 0 \\ &\vdots \\ &\vdots \\ T_{k-1}^p \exp\left[\frac{\mu\Delta x_{k-1}}{R(x_k)}\mathcal{S}_{k-1}^p\right] - T_k^p &= 0 \quad \ldots k-1 \text{ eqns.} \end{aligned} \tag{21}$$

$$\begin{aligned} &u_2^p - \frac{R(x_1)}{K\mu}\mathcal{S}_1^p T_1^p\left[\exp\left(\frac{\mu\Delta x_1}{R(x_1)}\mathcal{S}_1^p\right) - 1\right] = g_{id}(t_p) \\ &u_3^p - u_2^p - \frac{R(x_2)}{K\mu}\mathcal{S}_2^p T_2^p\left[\exp\left(\frac{\mu\Delta x_2}{R(x_2)}\mathcal{S}_2^p\right) - 1\right] = 0 \\ &\vdots \\ &\vdots \\ &u_k^p - u_{k-1}^p - \frac{R(x_{k-1})}{K\mu}\mathcal{S}_k^p T_{k-1}^p\left[\exp\left(\frac{\mu\Delta x_{k-1}}{R(x_{k-1})}\mathcal{S}_k^p\right) - 1\right] = 0 \\ &u_k^p + \frac{T_k^p}{2}\frac{\Delta x_k}{K} = u_{k+1}^{p-1} - \frac{T_{k+1}^{p-1}}{2}\frac{\Delta x_k}{K} \quad \ldots k \text{ eqns.} \end{aligned} \tag{22}$$

With the boundary conditions imposed by the actuating motion of the end of the cable, $u(x_1,t_p) = g_i d(t_p)$, and stationary node $k+1$, $u(x_{k+1},t_p) = u(x_{k+1},t_p - 1)$, the motion of all the intermediate nodes $u(x_2,t_p)$, $u(x_2,t_p)$,. . ., $u(x_k,t_p)$ are unknown (k – 1 unknowns). In addition, tension of the first k nodes $T(x_1,t_p)$, $T(x_2,t_p)$, . . ., $T(x_k,t_p)$ are unknown (k unknowns), the tension of node $k + 1$ being known from previous time step. Therefore, these $2k$ – 1 unknown displacement and tension variables can be calculated by simultaneously solving the $2k$ – 1 equations in (21) and (22). The kth cable segment starts to move, and node k + 1 becomes the last moving node at time t_q when the following condition is satisfied:

$$T(x_{k+1}, t_{q-1})\,\mathcal{S}_k^p \geq T(x_k, t_q)\,\mathcal{S}_k^p \exp\left[\frac{\mu\Delta x_k}{R(x_k)}\mathcal{S}_k^p\right]. \tag{23}$$

As the nodes at x_1 and x_{n+1} keep on moving, tension at the input ends keep on changing, and motion propagates along the two cables A and B. Eventually, the last moving nodes of both the cables coincide and the cables start to move *en masse*. Apart from computational perspective, the concept of last moving node also helps us in physically analyzing the partial motion transmission across the cable. This becomes particularly useful for understanding the coupled motion transmission in a two-cable system, where one cable starts pulling another cable, as elaborated upon later in this section. If, at any point in time, tension on one of the cables becomes zero (cable goes slack), e.g., cable B, only the nodes of the other cable, as well as the distal node of the slack cable (i.e., node 1, 2,. . . , n, $2n$ in this case), need to be solved for motion transmission.

Since the motion of two cables are constrained by the pulleys connecting them, assuming no slacking at the two pulleys

$$\begin{aligned} u(x_n, t) - u(x_{2n}, t) &= 2R_o\theta_o \\ u(x_n, t) + u(x_{2n}, t) &= 2L. \end{aligned} \tag{24}$$

Simulations are carried out assuming negligible friction losses at the pulleys as compared with the losses in the conduits. Thus, the boundary condition in (8) can be simplified as follows:

$$\tau_o = -K_e\theta_o = (T_2 - T_4)R_o \tag{25}$$

where τ_o is the external torque being applied by the load, θ_o is its angular rotation at the output, R_o is the radius of the pulley attached to the load motor, K_e is the simulated environment stiffness, $2L$ is the sum of two conduit lengths corresponding to cables A and B, and T_k (k = 1, 2, 3, 4) denote the tension at the two ends of each cable, i.e., $T_1(t) = T(x_1,t)$, $T_2(t) = T(x_n,t)$, $T_3(t) = T(x_{n+1},t)$, and $T_4(t) = T(x_{2n}, t)$.

The input motor is simulated to follow a sinusoidal oscillatory motion profile. At each time step, based on the aforementioned discussion, the last moving node of each cable is estimated for the given input motion. The tension and displacements of all the nodes up to the last moving node are calculated accordingly. If one of the cables goes slack, the parameters for the other cable are calculated as an independent cable with the corresponding load, since the slack cable no longer affects its motion. Based on the earlier analysis, the motion of the system can be divided in two categories: 1) both cables taut or 2) either cable slack.

Simulations are carried out for the two-cable system, where each cable is of length 2 m, looped thrice, with a pretension of T_0 = 10 N; the equivalent stiffness of the cable-conduit system is 1 kN/m, and the environment stiffness is 0.4 kN·m. The cables are divided in 16 sections each, and a time step of 0.25 ms was used for the simulations. A sinusoidal motion of amplitude 1 rad and frequency of 1 Hz is applied as the input. Simulation results are shown in Fig. 5. Various time instants have been marked by numbers to facilitate the comparison of various parameters as well as correlating the trends in different plots. For simplicity, time instant 1 has been chosen when the direction of motion changes for the first time. The tension transmission across the two cables, i.e., cable A and cable B, is shown in Fig. 5(a) and (b), respectively. Although the tension transmission profiles are largely similar to the case of single cable transmission, differences due to cable coupling are visible as "peaks" in the transmission profile (highlighted by the dotted circle), which are discussed in detail later in the section as phase II (one cable pulling another cable). The overall tension profiles

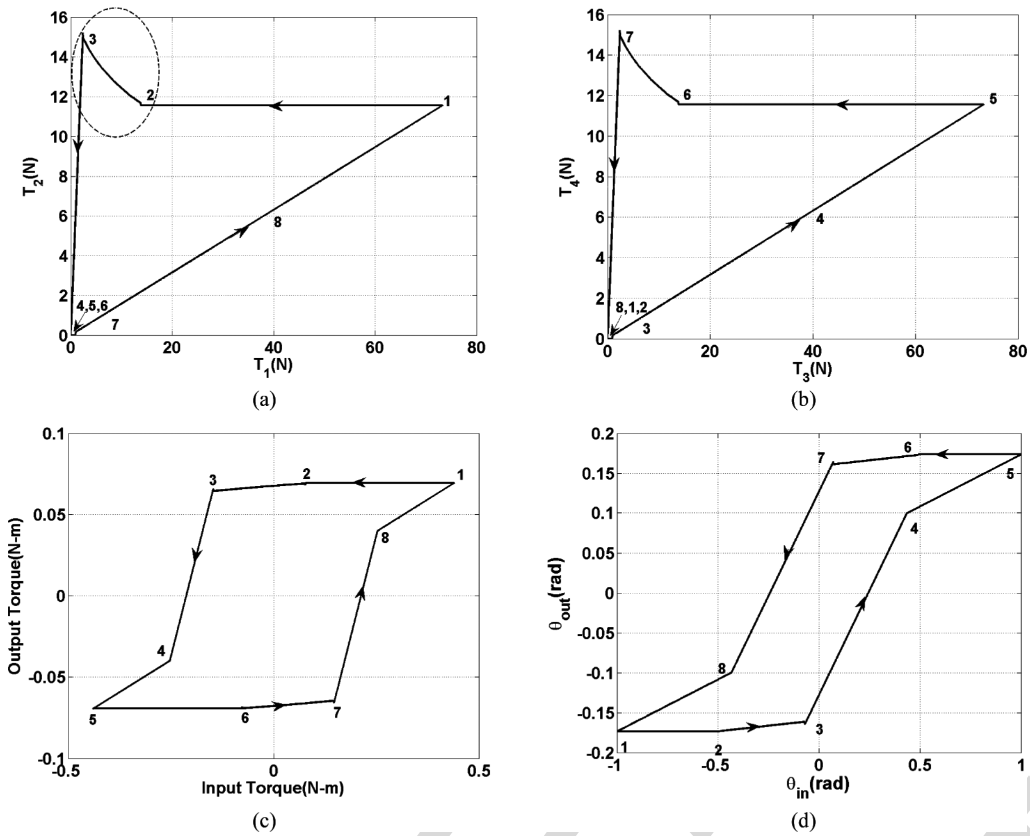

Fig. 5. *Transmission profile* with various time instants. (a) Tension transmission across cable A (T_1 versus T_2) and (b) across cable B (T_3 versus T_4). (c) Torque transmission from the actuator ($\tau_{\rm in}$) to the load ($\tau_{\rm out}$). (d) Angular rotation transmission from the drive pulley ($\theta_{\rm in}$) to the follower pulley ($\theta_{\rm out}$).

are similar for the two cables, as shown in Fig. 5(a) and (b), however, with different states at any time instant.

Apart from comparing the tension variation, in the case of the two-cable system, we can also compare torque and angular motion transmission from the actuator to the load. The torque transmission is shown in Fig. 5(c), and the angular motion propagation is shown in Fig. 5(d). Both the torque and motion transmission follow a backlash type of profile, however, with different slopes and widths.

To understand the mechanism of motion propagation across the cable, consider Fig. 6, showing the variation of output torque versus input torque ($\tau_{\rm in}$ versus $\tau_{\rm out}$). The transmission profile can be divided in various phases, as marked in the figure. These phases can be briefly described as follows.

1) *Output pulley not moving:* When the motion has not propagated to the distal end of either of the two cables (i.e., the output load), both the cables move independently, and as a result, no torque is transmitted to the output, and the output pulley does not move. This corresponds to the width of the backlash, as represented by the flat sections (time intervals 1–2 and 5–6 in Fig. 5).

2) *One cable pulling another cable:* Because of difference in tension across the two cables, friction levels are also different, and as a result, the rate of motion propagation varying across the two cables is also different. Therefore, there are time instances when motion propagates to the end of only one cable (without loss of generality assume cable A), while the other cable (cable B) is partially moving. Thus, cable A is causing the output pulley to move, as well as the distal end of cable B, while the (partial) motion of the drive end of cable B does not influence the motion of the load pulley. This gives rise to the section with small slope in the backlash profile (time intervals 2–3 and 6–7), since only one cable is active in motion transmission to the load, which is also referred to as soft spring [12]. In

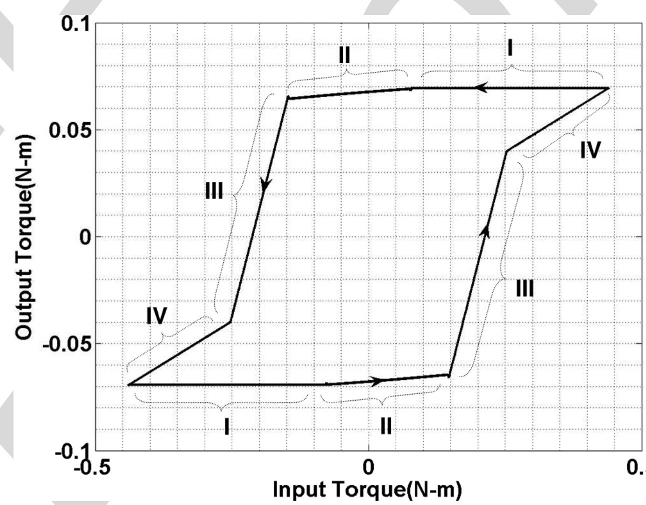

Fig. 6. Torque transmission profile.

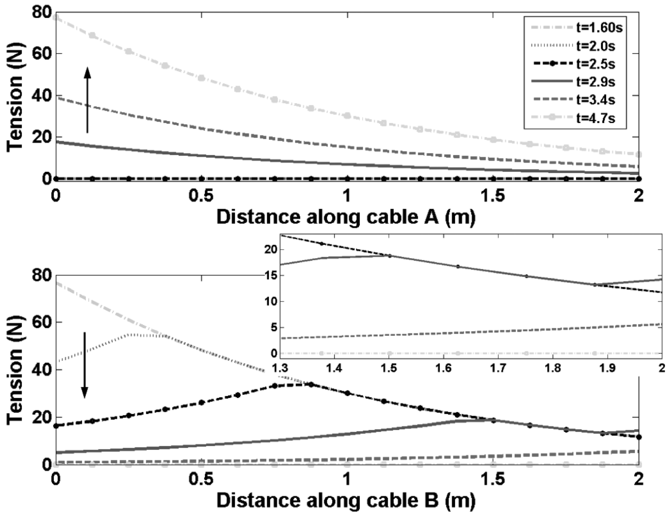

Fig. 7. Tension variation across the length of the two cables.

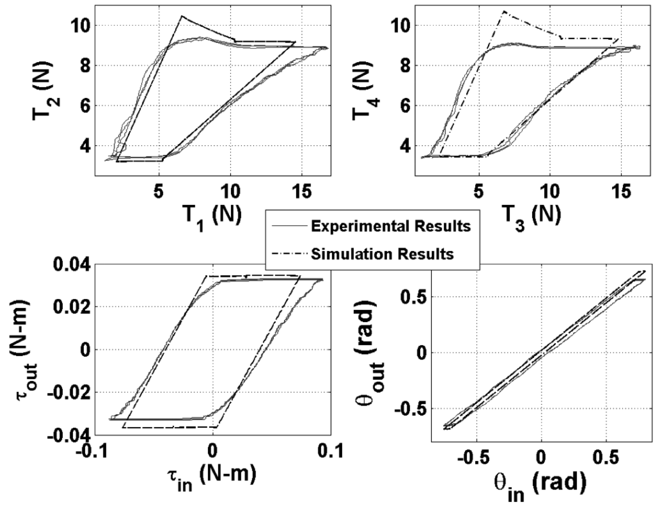

Fig. 8. Experimental and simulation results for $T_0 = 7.3$ N, using the original parameter estimates.

the tension transmission profile, this gives rise to the phase when (in cable B); although the tension at the drive end of the cable is decreasing, the tension at the follower end is increasing (due to pulling by cable A), as shown by the solid brown line in Fig. 7 and dotted circle in Fig. 5(a). Thus, the interaction between the two cables gives rise to these *counter-intuitive* peaks in tension transmission profile, which is not visible in the case of single cable.

3) *Both cables moving:* When the last moving nodes of both the cables coincide, both the cables collectively move, transmitting torque to the output, which corresponds to the slope of the backlash in the torque as well as motion transmission (time intervals 3–4 and 7–8).

4) *One cable slack, while other cable is moving:* Depending on the input motion profile and the pretension, large tension drop across one of the cable can lead to cable slacking, while the tension across the other cable increases, and it keeps moving. This decreases the slope of the backlash, since only one cable is effectively transmitting motion, and hence, the apparent stiffness of the system reduces (time intervals 8–1 and 4–5). This phase can be further subdivided into two cases: a) Motion of the drive pulley continues in the same direction, and b) drive pulley changes its direction of motion.

These four phases define the cable motion. While phases I and II are generally of short time duration, phases III and IV govern the motion during most of the operation. Note that the occurrence and strength of all these phases are dependent on cable pretension as well as the amplitude of the input motion, apart from physical parameters of the system like cable length, stiffness, friction level, and environmental stiffness. From these plots, it is evident that friction not only causes a backlash type of transmission profile but also leads to other phenomenon, such as changes in the slope of the transmission due to cable slacking, introduction of small slopes in the torque transmission, as well as opposite tension variations at two ends of the cable due to partial motion propagation.

V. Experimental Results

To validate our simulation, experiments were performed using the setup described in Section II. The actuation cables were 0.52 mm in diameter, uncoated stainless steel 7 × 19 wire rope that is approximately 1.6 m in length and wrapped around 12-mm-diameter motor pulleys. The stainless steel conduits were 1.2 m in length, made from 0.49-mm-diameter wire wrapped into a close-packed spring with an inner diameter of 1.29 mm. The two motors were controlled using the dSpace control board. For this study, the pretension in the cables and shape of the conduit could be varied and controlled. Pulley rotation was measured with a resolution of 0.18°. Pulley torque was measured with an accuracy of 0.1 mN·m over a range of 100 mN·m, while the combined cable tension measured by the load cell had an accuracy of 0.1 N over a range of 45 N.

To correlate the experimental results with the simulation, several system properties were experimentally estimated. In particular, the stiffness of the cable and conduits were measured to be 15.43 and 137.76 kN/m, respectively. Since the cable and the conduits act as springs in parallel, the equivalent cable stiffness was calculated to be 13.88 kN/m. Force relaxation or the creep of the cable was measured to be approximately 10.5%, with a time constant of approximately 30 s and, therefore, deemed negligible for these initial experiments. The friction coefficient between the cable and the conduit was measured to be 0.147, and the viscous friction was negligible and could be ignored as experimental error.

Fig. 8 shows the experimental and simulation results for a half loop in the conduit. The pretension in the experiments was approximately set at $T_0 = 7.3$ N, applying a uniform pretension across the cable not being possible due to the friction effects. The simulations capture all the major trends observed in experiments and match the numbers closely. In the experimental results, for the tension transmission profile, we observe a hump or a peak as predicted by the simulations. In addition, the

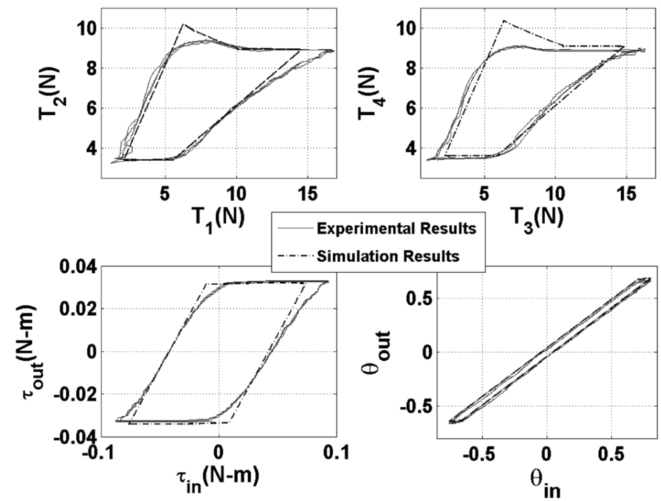

Fig. 9. Fitting of experimental results and simulation results for the recalculated cable parameter $k = 7.5$ kN/m, and $\mu = 0.156$.

TABLE I
NORMALIZED ERROR PERCENTAGE

	θout	*τ_in*	*τ_out*	*T₁*	*T₂*	*T₃*	*T₃*
R.M.S.E. (%)	3.7	19.4	3.7	12.8	4.1	9.9	5.5

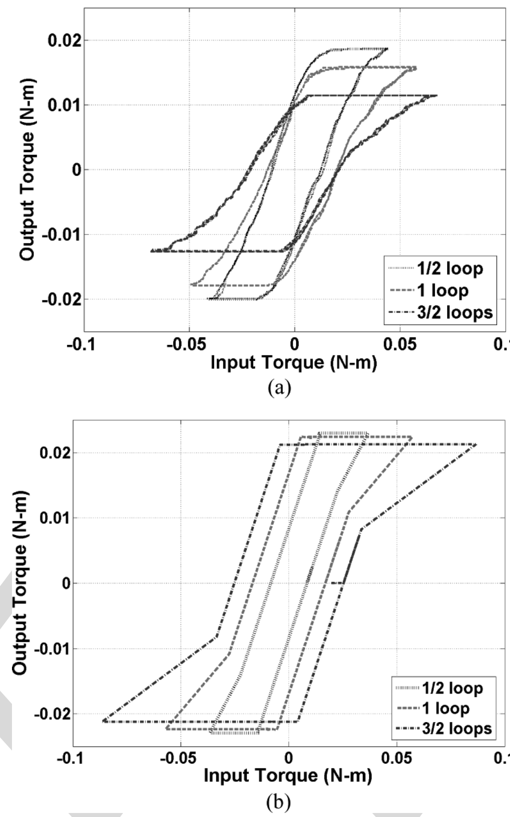

Fig. 10. Variation in torque transmission with number of loops. (a) Experimental results for different number of loops in conduit. (b) Simulation results for corresponding number of loops.

backlash in the torque and motion transmission is similar to what is predicted in the simulation results.

To analyze, goodness of fit between simulation and experimental results, the model was fitted on the experimental data to back calculate the cable stiffness and friction coefficients as 7.75 kN/m and 0.156, respectively. Using these parameters, the simulations were carried out again and compared with experimental results, as shown in Fig. 9. Table I shows the normalized rms percentage over one cycle for various parameters.

In the following sections, the effect of variation in cable pretension and conduit path has been studied, and the change of behavior as captured by simulations and experiments are compared.

A. Variation of Conduit Path

Friction is exponentially correlated to the angle of curvature of the conduit. Thus, increasing the curvature angle should increase the friction and, hence, larger backlash width. Larger friction also leads to longer time periods when one of the cables is slack, while the other cable is moving (phase IV), as well as smaller slope during this phase. To verify this, the curvature angle of the conduit is varied, while all the other parameters are kept constant, and its effect on the transmission profile is observed. For simplicity, the conduit shape was changed by adding additional ''*half-loops*'' or *180*° of bend. For introducing loops, the entire length of the conduits was used such that the radius of curvature remained constant throughout the conduit. To maintain uniformity in pretension, cables were loaded after changing the number of loops. The simulation results in Fig. 10(b) match well with the experimental results in Fig. 10(a). An increase in the backlash width, as well as change in the slope, as seen in experimental results, have been well predicted by the simulations.

B. Variation of Pretension

Since, according to (2), the tension loss is directly proportional to pretension, increasing the pretension increases the backlash. For a large pretension of 7 N, cables do not slack, and therefore, phase IV is not present. For a pretension of 3.5 N, phase IV is present, when one cable goes slack, while the other is still moving. This is also visible for the pretension of 0.7 N, but in this case, an additional trend is present, showing the second case of phase IV when one cable remains slack, while the other cable is moving, and the input switches its direction of motion. Experimental results in Fig. 11(a) show the change in the backlash width as well as cable slacking (both phase IVa and IVb), which can also be observed in simulation results in Fig. 11(b).

C. Variation of Loop Radius

According to (4), tension variation across the cable is related to $\Delta x/R \doteq \Delta\theta$. Therefore, for a constant angle of curvature $\Delta\theta$, the model predicts that there is no effect on system behavior with a change in the radius of curvature. To verify this, experiments were carried out for three different loop radii of 4.57, 6.35, and 7.62 cm (1.8, 2.5, and 3 in), while keeping the curvature angle

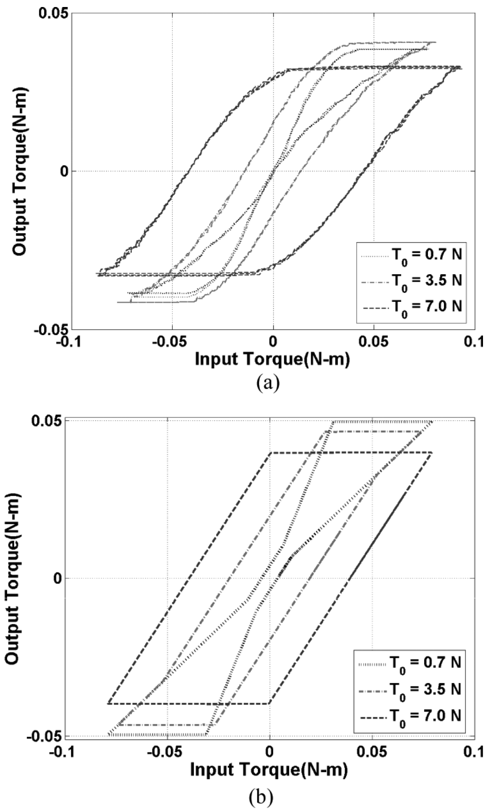

Fig. 11. Variation in torque transmission with pretension in the cables. (a) Experimental results for different cable pretension. (b) Simulation results for corresponding variation in pretension.

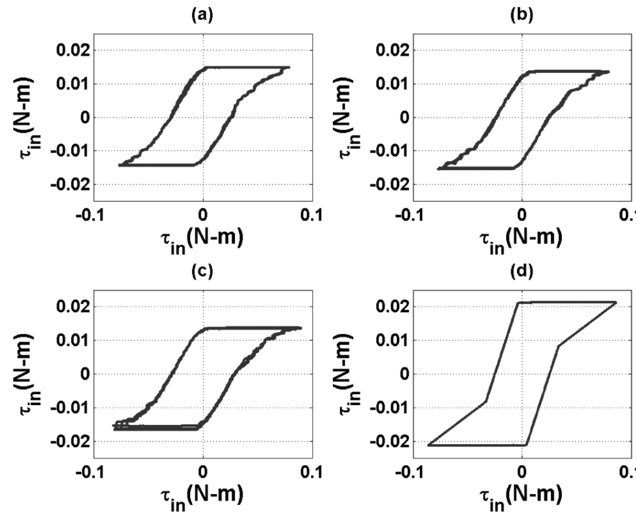

Fig. 12. Variation in torque transmission with loop radius. Experimental results for loop radius (a) 4.57 cm, (b) 5.35 cm, (c) 7.62 cm, and (d) corresponding simulation result.

same. Constant radius was implemented by wrapping the conduit around a circular object. Similar to Section V-A, pretension was applied after changing the number of loops. Corresponding experimental torque profiles are shown in Fig. 12(a)–(c), while the simulation result is shown in Fig. 12(d). From the plots, it can be inferred that the variation with the loop radius is minimal, as predicted by the model.

VI. Conclusion

Although using a pair of cables in pull–pull configuration provides simple and cost-effective power transmission in a surgical robot as well as other robotic devices, its use has been limited due to the nonlinearities generated due to friction and compliance present in the system. A system model was needed to analyze the nonlinearities in the system and to understand the tradeoffs involved arising from tension losses and cable slacking due to friction. While transmission models have been developed earlier, their application scope was quite restricted due to the assumptions of single-cable transmission, constant curvature, and cable pretension.

In this paper, starting from the system dynamics, we have developed a discretized model of the transmission characteristics of the system. The model has been validated on the experimental setup developed, which emulates a typical robot actuation. Simulations were successful not only in predicting the trends of the transmission characteristics in the experimental setup but in the magnitudes of various parameters with high accuracy as well. The differences in experimental and simulation results can be attributed to various approximations inherent in the system modeling, experimental errors, as well as errors in system parameter identification. Although due care was taken, kinks may have been inadvertently introduced in the cables, which also deteriorate the system performance.

For the modeling cable inertia that has been neglected, typical cable mass is less than 2 gm/m for the steel cables used. However, at extremely low-tension levels and inflection or singularity points in motion trajectory, inertia may not be negligible. The simulations use static Coulomb friction model. Using a dynamic friction model, like Dahl's friction model, may provide better results. The use of Coulomb friction model, together with negligible inertia, might be the reason of sharp transition in simulations, which are not present in the experimental results. The model also neglects the effects of force relaxation and friction effects at the two pulleys. Although placement of the loop along the conduit has not been explicitly discussed, the model captures its effects by appropriately defining the conduit curvature. Loop placement does not directly change the capstan effect; however, it changes the cable elongation and, therefore, also changes the overall transmission profile.

Although the environmental load has been assumed as a torsional spring, it can be conveniently modified for a generic load in (25). Although corresponding simulations have not been carried out, the results are expected to follow a similar friction dependent backlash-type behavior, since the deadband is dependent on friction due to cable pretension and not on the external load. For the experiments, a constant radius has been used. However, in practice, various sensors, e.g., fiber optic sensors can be placed along the conduit, which can be used to estimate the conduit curvature. The model can be further improved by incorporating the load dynamics. The current model assumes high-conduit bending stiffness and does not model the changes in pretension, which occur due to the changes in the path of conduit due to lateral forces exerted by the cable.

This system model, while reinforcing the results obtained in other publications, also bring up some key phenomena not observed earlier, particularly due to cable coupling. An attempt has been made to duly highlight all these aspects using the simulation results. Apart from torque transmission, motion transmission, which is necessary for position control, has also been presented, which was completely ignored in previous work. Furthermore, due analysis has been done to highlight all the physical parameters, as well as experimental conditions, which affect the motion transmission. Since the model has been validated, in the future, this model can be used to develop new control strategies for both force control as well as position control. An effective controller implementation can lead to active usage of cable drives in robotic systems, particularly in surgical robots, where the cable conduits can bring dexterity and flexibility in laparoscopic surgical robots, which the current systems lack.

REFERENCES

[1] V. Agrawal, W. J. Peine, and B. Yao, "Modeling of closed loop cable-conduit transmission system," in *Proc. IEEE Int. Conf. Robot. Autom.*, Pasadena, CA, May 2008, pp. 3407–3412.

[2] G. S. Guthart and J. K. Salisbury, "The intuitive telesurgery system: Overview and applications," in *Proc. IEEE Int. Conf. Robot. Autom.*, San Francisco, CA, Apr. 2000, pp. 618–621.

[3] R. J. Fanzino, "The Laprotek surgical system and the next generation of robotics," *Surg. Clin. N. Amer.*, vol. 83, no. 6, pp. 1317–1320, Dec. 2003.

[4] L. Biagiotti, F. Lotti, C. Melchiorri, G. Palli, P. Tiezzi, and G. Vassura, "Development of UB hand 3: Early results," in *Proc. IEEE Int. Conf. Robot. Autom.*, Barcelona, Spain, Apr. 2005, pp. 4488–4493.

[5] F. Lotti and G. Vassura, "A novel approach to mechanical design of articulated finger for robotic hands," in *Proc. IEEE/RSJ Int. Conf. Intell. Robots Syst.*, Lausanne, Switzerland, Oct. 2002, pp. 1687–1692.

[6] A. Nahvi, J. M. Hollerbach, Y. Xu, and I. W. Hunter, "Investigation of the transmission system of a tendon driven robot hand," in *Proc. IEEE Int. Conf. Intell. Robots Syst.*, Munich, Germany, Sep. 1994, vol. 1, pp. 202–208.

[7] I. Kassim, W. S. Ng, G. Feng, S. J. Phee, P. Dario, and C. A. Mosse, "Review of locomotion techniques for robotic colonoscopy," in *Proc. IEEE lnt. Conf. Robot. Autom.*, Taipei, Taiwan, Sep. 2003, pp. 1086–1091.

[8] S. J. Phee, W. S. Ng, I. M. Chen, F. Seow-Choen, and B. L. Davies, "Locomotion and steering aspects in automation of colonoscopy," *Eng. Med. Biol. Mag., IEEE*, vol. 16, no. 6, pp. 85–96, Nov./Dec. 1997.

[9] J. F. Veneman, R. Ekkelenkam, R. Kruidhof, F. C. T. van der Helm, and H. Van Der Kooij, "Design of a series elastic- and Bowden-cable-based Actuation system for use as torque actuator in exoskeleton-type robots," *Int. J. Robot. Res.*, vol. 25, no. 3, pp. 261–281, 2006.

[10] A. Schiele, P. Letier, R. van der Linde, and F. Van Der Helm, "Bowden Cable actuator for force-feedback exoskeletons," in *Proc. IEEE Int. Conf. Intell. Robot. Syst.*, Beijing, China, Oct. 2006, pp. 3599–3604.

[11] A. Schiele, "Performance difference of Bowden Cable relocated and non-relocated master actuators in virtual environment applications," in *Proc. IEEE Int. Conf. Intell. Robots Syst.*, Nice, France, Sep. 2008, pp. 3507–3512.

[12] M. Kaneko, W. Paetsch, and H. Tolle, "Input-dependent stability of joint torque control of tendon-driven robot hands," *IEEE Trans. Ind. Electron.*, vol. 39, no. 2, pp. 96–104, Apr. 1992.

[13] W. T. Townsend and J. K. Salisbury, Jr., "The effect of coulomb friction and stiction on force control," in *Proc. IEEE Int. Conf. Robot. Autom.*, Mar. 1987, vol. 4, pp. 883–889. Q4

[14] M. Kaneko, T. Yamashita, and K. Tanie, "Basic considerations on transmission characteristics for tendon drive robots," in *Proc. Int. Conf. Adv. Robot.*, 1991, vol. 1, pp. 827–832.

[15] M. Kaneko, M. Wada, H. Maekawa, and K. Tanie, "A new consideration on tendon tension control system of robot hands," in *Proc. IEEE Int. Conf. Robot. Autom.*, Sacramento, CA, 1991, vol. 2, pp. 1028–1033.

[16] G. Palli and C. Melchiorri, "Model and control of tendon-sheath transmission systems," in *Proc. IEEE Int. Conf. Robot. Autom.*, 2006, pp. 988–993. Q5

[17] G. Palli and C. Melchiorri, "Optimal control of tendon-sheath transmission systems," in *Proc. IFAC Symp. Robot Control*, 2006.

Authors' photographs and biographies not available at the time of publication.

QUERIES

Q1: Author: Please check the IEEE membership information of the authors as the membership of the first two authors was mentioned only in the transmittal PDF and not in the original manuscript. Checked

Q2: Author: Please check and confirm footnote first as typeset.

Q3. Author: Please spell out ‘PTFE’ in full, if possible. Polytetrafluoroethylene

Q4. Author: Please check Ref. [14] as typeset. Spelling of "transmission" to be corrected in the title, typeset checked.

Q5. Author: Please provide page range for Ref. [17].

Ref. [17] should be updated as:
G. Palli and C. Melchiorri, "Optimal Control of tendon-sheath transmission systems,"
in Proc. 8th Int. IFAC Symp. Robot Control, Bologna, Italy, Sep 2006, vol. 8, no. 2, pp. 185-191